

JPRS-UPM-91-003  
7 MARCH 1991



# *JPRS Report*

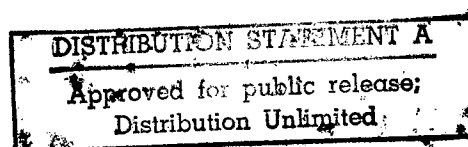
# Science & Technology

## *USSR: Physics & Mathematics*

DTIC QUALITY INSPECTED 2

REPRODUCED BY  
U.S. DEPARTMENT OF COMMERCE  
NATIONAL TECHNICAL INFORMATION SERVICE  
SPRINGFIELD, VA. 22161

19990305 051



# Science & Technology

## USSR: Physics & Mathematics

JPRS-UPM-91-003

CONTENTS

7 MARCH 1991

### Acoustics

Acoustic Shock Waves in Magnetic Materials With Plane of Easy Magnetization [A. F. Kabychenkov, V. G. Shavrov, et al.; FIZIKA TVERDOGO TELA, Vol 32 No 7, Jul 90] .....	1
Formation of Cumulative Quasi-Spherical Converging Shock Wave Upon Reflection of Toroidal Shock Wave by Hard Surface [E. M. Barkhudarov, M. O. Mdivnishvili, et al.; PISMA V ZHURNAL EKSPERIMENTALNOY I TEORETICHESKOY FIZIKI 10 Oct 90] .....	1
Method of Describing Shock Wave Sensitivity of Solid Explosives [A. V. Dubovik; FIZIKA GORENIYA I VZRYVA, Vol 26 No 4, Jul-Aug 90] .....	1
Relation Between Parameters of Normal Detonation and Heat of Explosion of Condensed Explosives [B. A. Sokolov, V. S. Trofimov; FIZIKA GORENIYA I VZRYVA, Vol 26 No 4, Jul-Aug 90] .....	2
Effect of Shock Wave and Subsequent Quenching in Stream of Coolant on Y-Ba-Cu-O Ceramic [D. L. Guryev; FIZIKA GORENIYA I VZRYVA, Vol 26 No 5, Sep-Oct 90] .....	2
Mechanism of Secondary Blast Waves Behind One-Dimensional Detonation Wave in Gas [S. M. Aksamentov, D. I. Matsukov, et al.; FIZIKA GORENIYA I VZRYVA, Vol 26 No 5, Sep-Oct 90] ..	2
New Method of Calculating Normal Waves in Acoustic Waveguides [A. M. Zhelvis, Ye. A. Rivelis, et al.; AKUSTICHESKIY ZHURNAL, Vol 36 No 4, Jul-Aug 90] .....	3
Use of Acoustic Sounding for Determination of Aerosol Parameters [B. Ye. Nemtsov; AKUSTICHESKIY ZHURNAL, Vol 36 No 4, Jul-Aug 90] .....	3
Solitary Wave in Thin Uniformly Curvilinear Beam [S. A. Rybak, Yu. I. Skrynnikov; AKUSTICHESKIY ZHURNAL, Vol 36 No 4, Jul-Aug 90] .....	3
Fast Algorithm of Eigenvalue Calculation for Absorbing Multilayer Waveguide [G. V. Alekseyev, Ye. G. Komarov; AKUSTICHESKIY ZHURNAL, Vol 36 No 6, Nov-Dec 90] .....	4
Explosive Boiling and Generation of Shock Waves in Biotissue During Ablation by CO <sub>2</sub> Laser Pulses [A. K. Dmitriyev, N. P. Furzikov; AKUSTICHESKIY ZHURNAL, Vol 36 No 6, Nov-Dec 90] .....	4
Propagation of Undistorted Compression Shock Through Nonlinear Standard Viscoelastic Medium [A. S. Stulov; AKUSTICHESKIY ZHURNAL, Vol 36 No 6, Nov-Dec 90] .....	4

### Crystals, Laser Glasses, Semiconductors

Gas-Sensitive Effects in Structures Based on Semiconductor Oxide Systems V <sub>2</sub> O <sub>5</sub> -SnO <sub>2</sub> [A. S. Tonkoshkur, I. M. Chernenko; ZHURNAL TEKHNIЧЕСКОY FIZIKI, Vol 60 No 8, Aug 90] ...	6
Optical Properties of New Ferroelastic Materials [NH <sub>2</sub> (C <sub>2</sub> H <sub>5</sub> ) <sub>2</sub> ] <sub>2</sub> MCl <sub>4</sub> (M = Cu, Co) [O. G. Blokh, M. I. Bublyk, et al.; PISMA V ZHURNAL TEKHNIЧЕСКОY FIZIKI 12 Aug 90] .....	6
Optical Properties of the New Ferroelastics [NH <sub>2</sub> (C <sub>2</sub> H <sub>5</sub> ) <sub>2</sub> ] <sub>2</sub> CuCl <sub>4</sub> and [NH <sub>2</sub> (C <sub>2</sub> H <sub>5</sub> ) <sub>2</sub> ] <sub>2</sub> CoCl <sub>4</sub> [O. G. Blokh, M. I. Bublyk, et al.; PISMA V ZHURNAL TEKHNIЧЕСКОY FIZIKI 12 Aug 90] .....	6
Use of Honeycomb Structures and Polycrystalline Diamond Films in Anodes for Soft X-Ray Sources [A. M. Prokhorov, I. N. Sisakin, et al.; PISMA V ZHURNAL TEKHNIЧЕСКОY FIZIKI 12 Aug 90] ..	6

### Fluid Dynamics

Half-Quantum Vortices in Superfluid <sup>3</sup> He-B [G. Ye. Volovik; PISMA V ZHURNAL EKSPERIMENTALNOY I TEORETICHESKOY FIZIKI 25 Sep 90] ..	7
Structure of Surface Layer in Superfluid <sup>3</sup> He-B [G. Ye. Volovik; PISMA V ZHURNAL EKSPERIMENTALNOY I TEORETICHESKOY FIZIKI 25 Sep 90] ..	7
Effect of Dissipation on Structure of Stationary Wave Turbulence Spectrum [I. V. Ryzhenkova, G. Ye. Falkovich; ZHURNAL EKSPERIMENTALNOY I TEORETICHESKOY FIZIKI, Vol 98 No 6(12), Dec 90] .....	7
Generation, Annihilation, and Soliton-Like Passage of Vertical Bloch Line Clusters in Domain Wall of Ferromagnet [Ye. Ye. Kotova, V. M. Chetverikov; ZHURNAL EKSPERIMENTALNOY I TEORETICHESKOY FIZIKI, Vol 98 No 6(12), Dec 90] .....	8

Effect of Crystal Structure Characteristics on Magnetic Properties of $\text{Nd}_2\text{CuO}_4$ [V. A. Blinkin, I. M. Vitebskiy, et al.; ZHURNAL EKSPERIMENTALNOY I TEORETICHESKOY FIZIKI, Vol 98 No 6(12), Dec 90] .....	8
---	---

**Lasers**

Collective Induced Radiation of Spatially Limited Groups of Electron Oscillators: Channeling and Superradiant Radiation [N. S. Ginzburg, A. S. Sergeev; ZHURNAL TEKHNICHESKOY FIZIKI, Vol 60 No 8, Aug 90] .....	9
Aberration Thermocapillary Transformation of Laser Beams [S. A. Viznyuk, S. F. Rastopov, et al.; ZHURNAL TEKHNICHESKOY FIZIKI, Vol 60 No 8, Aug 90] ..	9
Femtosecond Relaxation of Excited Carriers in $\text{CdSe}(x)\text{S}(1-x)$ Microcrystals Glass Matrix After High-Intensity Excitation [Yu. Ye. Lozovik, Yu. A. Matveyets, et al.; PISMA V ZHURNAL EKSPERIMENTALNOY I TEORETICHESKOY FIZIKI 25 Aug 90] .....	9
High-Speed X-Ray Electron-Optical Diagnostics of a Laser Plasma [V. K. Chevokin; KVANTOVAYA ELEKTRONIKA Vol 17 No 9, Sep 90] .....	10
A Free-Running and Q-Switched Erbium Mini-Laser [I. L. Vorobyev, V. P. Gapontsev, et al.; KVANTOVAYA ELEKTRONIKA Vol 17 No 9, Sep 90] .....	10
The Effect of Inter-Cavity Medium on Laser Mode Gain in a Wideband Laser [S. A. Kovalenko, S. P. Semin; KVANTOVAYA ELEKTRONIKA Vol 17 No 9, Sep 90] .....	10
Efficient Parametric Light Beam Amplification. I. Optimization of Parametrically-Amplified Interacting Wave Profiles [I. A. Begishev, A. A. Gulamov, et al.; KVANTOVAYA ELEKTRONIKA Vol 17 No 9, Sep 90] .....	10
A Dynamic Model of Active Mode Locking in a Gas Laser [L. A. Melnikov, G. N. Tatarkov; KVANTOVAYA ELEKTRONIKA Vol 17 No 9, Sep 90] .....	11
Laser Beams With Screw Dislocations of Wavefront [V. Yu. Bazhenov, M. V. Vasnetsov, et al.; PISMA V ZHURNAL EKSPERIMENTALNOY I TEORETICHESKOY FIZIKI 25 Oct 90] .....	11
On Ultimate Efficiency of Heavy Inert Atom Lasers With d-p Transitions [B. M. Berkeliyev, V. A. Dolgikh, et al.; KVANTOVAYA ELEKTRONIKA, Vol 17 No 12, Dec 90] .....	11
Optical Logic Elements for High-Throughput Optical Processors [V. B. Fedorov; KVANTOVAYA ELEKTRONIKA, Vol 17 No 12, Dec 90] .....	11
XeCl Laser Excited by Microwave Microsecond-Long Megawatt Pulses of a 3.07 GHz Industrial Microwave Oscillator [V. A. Vaulin, V. N. Slinko, et al.; KVANTOVAYA ELEKTRONIKA, Vol 17 No 12, Dec 90] .....	12
Vector Solitons in Fiber Optic Waveguide With Random Birefringence [Yu. S. Kivshar, V. V. Konotop; KVANTOVAYA ELEKTRONIKA, Vol 17 No 12, Dec 90] .....	12

**Nuclear Physics**

Solitons in Atomic Chain Under External Tension [R. Kh. Sabirov; FIZIKA TVERDOGO TELA, Vol 32 No 7, Jul 90] .....	13
Propagation of Solitons Within Phase Transition Range in External Field [V. I. Serikov, S. V. Voronin; FIZIKA TVERDOGO TELA, Vol 32 No 7, Jul 90] .....	13
Soliton and Domain Parts of Nonequilibrium Dielectric Permittivity of $\text{Rb}_2\text{ZnCl}_4$ [S. A. Gridnev, S. A. Prasolov, et al.; FIZIKA TVERDOGO TELA, Vol 32 No 7, Jul 90] .....	13
Possible Anomalous Interactions Between Ultracold Neutrons [V. A. Artyemyev; PISMA V ZHURNAL EKSPERIMENTALNOY I TEORETICHESKOY FIZIKI 25 Aug 90] ...	14
Interaction of Solitary Waves in System of Born-Infeld Equations [O. F. Menyshikh; TEORETICHESKAYA I MATEMATICHESKAYA FIZIKA, Vol 84 No 2, Aug 90] ...	14
Photoneutrino Production on Nuclei in Strong Magnetic Field [Yu. M. Loskutov, V. V. Skobelev; TEORETICHESKAYA I MATEMATICHESKAYA FIZIKA, Vol 84 No 2, Aug 90] .....	14
Another Contribution of Order $\alpha^2(Z\alpha)E_F$ to Hyperfine Split in Muonium and in Hydrogen [S. G. Karshenbaum, V. A. Shelyuto, et al.; PISMA V ZHURNAL EKSPERIMENTALNOY I TEORETICHESKOY FIZIKI 25 Sep 90] .....	15
Spontaneous Formation of Autosolitons in Stable Unbalanced Systems [B. S. Kerner, S. L. Klenov; PISMA V ZHURNAL EKSPERIMENTALNOY I TEORETICHESKOY FIZIKI 25 Sep 90] .....	15

Results of Measurements of Neutron Lifetime With Gravity Trap of Ultracold Neutrons [V. P. Alfimenkov, V. Ye. Varlamov, et al.; PISMA V ZHURNAL EKSPERIMENTALNOY I TEORETICHESKOY FIZIKI 10 Oct 90] .....	15
New Representation of Hubbard Model [G. G. Kahlullin; PISMA V ZHURNAL EKSPERIMENTALNOY I TEORETICHESKOY FIZIKI 10 Oct 90] ..	16
Charge Relaxation on Fractal Structures [V. Ye Arkhinchev; PISMA V ZHURNAL EKSPERIMENTALNOY I TEORETICHESKOY FIZIKI 10 Oct 90] .....	16
New Constraints on T-Invariance Breaking in $\beta$ -Decay [I. B. Khriplovich; PISMA V ZHURNAL EKSPERIMENTALNOY I TEORETICHESKOY FIZIKI 10 Nov 90] .	16
Limits on Neutrino Oscillation Parameters for Reactor Antineutrinos [G. S. Vidyakin, V. N. Vyrodov, et al.; ZHURNAL EKSPERIMENTALNOY I TEORETICHESKOY FIZIKI, Vol 98 No 3(9), Sep 90] .....	17
Masses of Quarks and Leptons in Model With Discrete Symmetry [N. I. Polyakov; PISMA V ZHURNAL EKSPERIMENTALNOY I TEORETICHESKOY FIZIKI 25 Nov 90] .	17
Phase Transitions and New Kinds of Ordering in Ising Model With Random-Field Defects [Ye. B. Kolomeyskiy; PISMA V ZHURNAL EKSPERIMENTALNOY I TEORETICHESKOY FIZIKI 25 Nov 90] .....	17

### Optics, Spectroscopy

Use of Multilayer Structures as Targets for Generating Collimated X-Ray Quantum Beams [Yu. I. Dudchik, F. F. Komarov, et al.; PISMA V ZHURNAL TEKHNIЧЕСKOY FIZIKI 12 Aug 90] .....	18
Fractal Characteristics of Percolation Conduction in Polycrystalline PbS Layers [O. A. Gudayev, V. K. Malinovskiy, et al.; PISMA V ZHURNAL EKSPERIMENTALNOY I TEORETICHESKOY FIZIKI 10 Sep 90] .....	18
Theory and Numerical Simulation of Optical Properties of Fractals [V. A. Markel, L. S. Muratov; ZHURNAL EKSPERIMENTALNOY I TEORETICHESKOY FIZIKI, Vol 98 No 3(9), Sep 90] .....	18
Generation of Nonlinear Surface Waves by Electromagnetic Beams [Ya. L. Bogomolov, A. V. Kochetov, et al.; ZHURNAL EKSPERIMENTALNOY I TEORETICHESKOY FIZIKI, Vol 98 No 4(8), Oct 90] .....	19
"Direct Viewing" of Atomic Structure of Crystal Under High-Resolution Electron Microscope [V. L. Indenbom, S. B. Tochilin; ZHURNAL EKSPERIMENTALNOY I TEORETICHESKOY FIZIKI, Vol 98 No 4(10), Oct 90] .....	19
Theory of Acceleration of Charged Particles by Ensemble of Shock Waves in Turbulent Medium [A. M. Bykov, I. N. Toptygin; ZHURNAL EKSPERIMENTALNOY I TEORETICHESKOY FIZIKI, Vol 98 No 4(10), Oct 90] .....	20
Control of Fermi Level and Phase Transitions in $YBa_2Cu_3O_{7-d}$ Material [Yu. M. Gerbshhteyn, N. Ye. Timoshchenko, et al.; ZHURNAL EKSPERIMENTALNOY I TEORETICHESKOY FIZIKI, Vol 98 No 4(10), Oct 90] .....	20

### Plasma Physics

Low-Frequency Potential Instabilities of Mutually Penetrating Electron Beams in Magnetic Gaps of Magnetoelectrostatic Traps [I. Ya. Gordiyenko, V. D. Yegorenkov, et al.; UKRAINSKIY FIZICHESKIY ZHURNAL, Vol 35 No 8, Aug 90] .	22
Substantiation of Quasi-One-Dimensional Bisoliton Model of Superconductivity of Ceramic Oxides [A. S. Davydov; UKRAINSKIY FIZICHESKIY ZHURNAL, Vol 35 No 8, Aug 90] .....	22
Magnetic Traps With Conductors "Floating" in Plasma [A. I. Morozov; PISMA V ZHURNAL TEKHNIЧЕСKOY FIZIKI 12 Aug 90] .....	22

### Superconductivity

Production and Atomic Structure of Single-Domain Tm-B-Cu-O Superconductor [V. I. Voronkova, V. K. Yanovskiy, et al.; PISMA V ZHURNAL EKSPERIMENTALNOY I TEORETICHESKOY FIZIKI 25 Aug 90] .....	23
Flux Creep and Depth of Pinning Centers in Organic Superconductor $k$ -(BEDT-TTF) $_2$ Cu(NSC) $_2$ [V. D. Kuznetsov, V. V. Metlushko, et al.; PISMA V ZHURNAL EKSPERIMENTALNOY I TEORETICHESKOY FIZIKI 10 Sep 90] .....	23

Critical Temperature for Ferromagnetic-Superconductor Superlattice [A. I. Buzdin, M. Yu. Kupriyanov; PISMA V ZHURNAL EKSPERIMENTALNOY I TEORETICHESKOY FIZIKI 10 Nov 90] FIZIKI 10 Nov 90] .....	23
Mechanism of Frozen Photoconductivity in $\text{YBa}_2\text{Cu}_3\text{O}_{7-d}$ Superconductor [I. P. Krylov; PISMA V ZHURNAL EKSPERIMENTALNOY I TEORETICHESKOY FIZIKI 25 Oct 90] .....	24
Low-Temperature Phase Transitions of First and Second Kinds in $\text{YBa}_2\text{Cu}_3\text{O}_{6+x}$ Due to Oxygen Redistribution Over Lattice Chains [L. G. Mamsurova, K. S. Pigalskiy, et al.; ZHURNAL EKSPERIMENTALNOY I TEORETICHESKOY FIZIKI, Vol 98 No 3(9), Sep 90] .....	24

#### Numerical Analysis, Algorithms

New Conformal Theories, "Magic" Level $k = 4$ , and Integrable Models [A. A. Belov, Yu. Ye. Lozovik; PISMA V ZHURNAL EKSPERIMENTALNOY I TEORETICHESKOY FIZIKI 10 Sep 90] .....	26
--	----

#### Differential Equations

Analog of Newton's Diagram for Class of Differential Equations With Singular Perturbation: Part 2 [G. S. Zhukova; DIFFERENTIALNYE URAVNIENIYA, Vol 26 No 9, Sep 90] .....	27
Class of Linear Differential and Discrete Games Between Groups of Pursuers and Evaders [N. Yu. Satimov, M. Sh. Mamatov; DIFFERENTIALNYE URAVNIENIYA, Vol 26 No 9, Sep 90] .....	27

UDC 537.634.2

### Acoustic Shock Waves in Magnetic Materials With Plane of Easy Magnetization

917J0005D Leningrad FIZIKA TVERDOGO TELA in Russian Vol 32 No 7, Jul 90 pp 2010-2014

[Article by A. F. Kabychenkov, V. G. Shavrov, and A. L. Shevchenko, Institute of Radio Engineering and Electronics, USSR Academy of Sciences, Moscow]

[Abstract] Propagation of low-frequency transverse acoustic waves through magnetic materials with a plane of easy magnetization and near its orientational phase transition is analyzed, once the propagation of longitudinal acoustic shock waves through ferroelectric materials at the Curie point had been analyzed (A. F. Kabychenkov and V. G. Shavrov, FIZIKA TVERDOGO TELA Vol 28 No 2, 1986). The analysis, in the quasi-static approximation, ignores not only nonuniform exchange interaction and spontaneous deformation as well as departure of magnetic moments  $M_1, M_2$  of the sublattices from the basis plane. An unbounded weak ferromagnetic medium is considered through which a transverse elastic wave propagates within the plane of easy magnetization in the direction of the external magnetic field. The case of a strong magnetic field is considered, where the strain amplitude is sufficiently small, but not too small, so that the wave propagates at different velocities through different segments and in the process becomes distorted owing to an increasing harmonic content in the increasingly nonlinear magnetoelastic vibrations. In a material near its orientational phase transition, the wave becomes distorted into one with a steeper leading edge and a flatter trailing edge. The coordinate of its discontinuity, the magnitude of the jump of elastic strain at that point, and the velocity of the resulting magnetoacoustic shock front are determined from the solution to the system of two equations describing the propagation of such a wave through such a medium with harmonic initial or boundary conditions. As orientational phase transition is approached, the shock front is formed within a shorter time or distance while the velocity of the trailing shock wave becomes equal to that of the original elastic wave and its amplitude decreases fast with increasing distance from the discontinuity point owing to dispersion and dissipation. The authors thank M. I. Kaganov and V. L. Preobrazhenskiy for discussion and helpful comments. References 4.

### Formation of Cumulative Quasi-Spherical Converging Shock Wave Upon Reflection of Toroidal Shock Wave by Hard Surface

917J0017D Moscow PISMA V ZHURNAL EKSPERIMENTALNOY I TEORETICHESKOY FIZIKI in Russian Vol 52 No 7, 10 Oct 90 pp 900-993

[Article by E. M. Barkhudarov, M. O. Mdivnishvili, I. V. Sokolov, M. I. Taktakishvili, and V. Ye. Terekhin, Institute of General Physics, USSR Academy of Sciences]

[Abstract] An experimental study has revealed a new kind of cumulative shock wave, a quasi-spherical converging one which forms upon reflection of a toroidal one by a hard surface. In the experiment, a shock wave in air under atmospheric pressure was generated by a toroidal gas-discharge plasma source with a radius  $R = 5$  cm receiving up to 1.3 kJ energy from the power supply. The generated toroidal shock wave, traveling with a velocity which reached 2 - 3 Mach on the inside circle nearest to the axis, struck a glass or plexiglass barrier which was movable so that the distance  $L$  traveled by this shock wave could be varied over the 1.5 - 5.5 cm range. A converging quasi-spherical shock wave was formed only when the torus-to-barrier distance was  $L \approx 0.7R \approx 3.5$  cm, evidently owing to an exceptionally strong one-shot heat effect under this condition. The results of this study are interpreted from the standpoint of the approximate Chester-Chisnell-Whitham theory, which yields  $N_{Ma}$  proportional to  $S^{-0.2}$  ( $S$  - area of shock wavefront). Pressure in the reflected shock wave was estimated in two ways, first, by reading the velocity on shadowgrams and second, by measuring the velocity of a plasticine ball 5 mm in diameter weighing 0.13 g shot by the quasi-spherical converging shock wave horizontally through a hole in the barrier at a height of 25 cm above the base. The shortest range of the ball trajectory was approximately 2 m and accordingly, the mean pressure exerted on the ball by that shock wave was approximately 100 atm. The authors thank G. A. Askaryan, I. A. Kossyy, and M. Vaselli for discussion. Figures 2; references 15.

UDC 534.222.2

### Method of Describing Shock Wave Sensitivity of Solid Explosives

917J0019A Novosibirsk FIZIKA GORENIYA I VZRYVA in Russian Vol 26 No 4, Jul-Aug 90 pp 98-101

[Article by A. V. Dubovik, Moscow]

[Abstract] The behavior of a porous explosive struck by a shock wave is described analytically, sliding friction in the slip planes being the principal mechanism by which such a substance is heated and then ignited. Randomness of grain orientation and nonrectilinearity of the trajectories of elementary shock perturbations are taken into account, displacements of grains therefore being mutually noncorrelated for at least a short initial period of time  $\tau \approx r/V$  ( $r$  - grain dimension,  $V$  - shock wave velocity in explosive medium) while any particular grains remain in rubbing for a period of time  $t_0 = d/u_0$  ( $d$  - pore dimension,  $u_0$  - shock wave velocity in pore) in a closed pore and  $t_0 = r/2u_0$  in an open pore. The temperature transient in the slip planes is calculated according to the Carslaw-Jaeger equation involving a shock wave as heat source and the explosive as a thermally active medium, the temperature rise above the initial ambient temperature being proportional to a finite time integral.

The time till adiabatic thermal explosion occurs is then calculated as a fraction of time  $t_0$  and with the critical pressure referred to that in a solid explosive. The mechanism of grain fracture in a shock wavefront is not definitively evident, cleavage appearing to be the most likely one. Further analysis and calculations are aided by data on relevant physical and chemical properties of TNT (2,4,6-trinitrotoluene), RDX (hexahydro-trinitro-triazine), and TEN (triethylamine). Figures 1; tables 1; references 7.

UDC 534.222.2

### Relation Between Parameters of Normal Detonation and Heat of Explosion of Condensed Explosives

917J0019B *Novosibirsk FIZIKA GORENIYA I VZRYVA in Russian Vol 26 No 4, Jul-Aug 90*  
pp 122-124

[Article by B. A. Sokolov and V. S. Trofimov, Chernogolovka]

[Abstract] The two relations for condensed explosives, for the rate of normal detonation  $D = (2k^2 - 2)^{1/2} Q_{ex}$  and for the pressure of combustion products at the Jouguet point  $p_1 = 2(k - 1)\rho_0 Q$  ( $k$  - polytropic exponent,  $Q_{ex}$  - heat of explosion measured with bomb calorimeter,  $\rho_0$  - initial density of explosive) are extended from ideal gases to any gaseous combustion products not necessarily having the same molecular mass and specific heat as the explosive. This is done by replacing  $Q$  by another appropriate quantity of heat which, in the general case, takes into account the isobaric-isochoric thermal and which will yield the exact value of  $D$  for the exact value of  $p_1$ . This new quantity of heat is shown to be  $Q = E - (p + p_0)(v_0 - v) / 2 - \Delta_1(p, v)$  ( $E = pv / (k - 1) + \Delta(p, v)$  - specific internal energy of combustion products). The relation between this new quantity and the calorimetrically determined heat of explosion then becomes  $Q = (k + 1)Q_{ex} / (3k - 1)$ . Calculations of  $D$  and  $p_1$  on this basis are compared with experimental data on  $D$  and  $p_1$  of 2,4,6-trinitrotoluene (TNT), hexahydro-trinitro-triazine (RDX), and TEN (triethylamine). Tables 1; references 4.

UDC 541.12.034.2

### Effect of Shock Wave and Subsequent Quenching in Stream of Coolant on Y-Ba-Cu-O Ceramic

917J0020A *Novosibirsk FIZIKA GORENIYA I VZRYVA in Russian Vol 26 No 5, Sep-Oct 90*  
pp 132-134

[Article by D. L. Guryev, Mendeleev]

[Abstract] An experimental study was made concerning the effect of a shock wave and subsequent quenching on the superconductor characteristics of orthorhombic  $YBa_2Cu_3O_x$ , the purpose of such a treatment being the retention of this metastable phase. Ceramic specimens

were produced from powder having a critical temperature of 91 K within a 1 K wide transition range. They were treated with shock waves with amplitudes of 100 - 160 GPa amplitude and adjustable velocity. Subsequent quenching in a stream of water relieved the shock-compressed state, nonadiabatically, first the temperature and then the pressure were lowered nonisentropically. Shock compression under a pressure of 104 GPa at an initial 291 K water temperature caused the material to break down into  $Y_2O_3$ ,  $Cu_2$ ,  $BaO$ ,  $BaCO_3$  in the final stage of the processes, this being possible only as a result of  $BaO$  interacting with water vapor and  $CO_2$  in the air. Quenching at 268 K improved the product and, by raising the pressure to 159 GPa, raised the  $BaCO_3$  content to 20 - 30 percent with retention of the orthorhombic phase. The product of shock treatment was compacted under a pressure of about 5 GPa into disks 5 mm in diameter. Electrical resistance measurements yielded the same 91 K critical superconducting transition temperature, but within a 10 K range, compaction of the original powder having had the identical effect. The authors thank O. Ye. Omelyanovskiy for supplying the original specimens and for performing the electrical resistance measurements, also L. I. Kopaneva and V. V. Gavryushin for performing their x-ray and elemental analysis. References 20.

UDC 534.222.2

### Mechanism of Secondary Blast Waves Behind One-Dimensional Detonation Wave in Gas

917J0020B *Novosibirsk FIZIKA GORENIYA I VZRYVA in Russian Vol 26 No 5, Sep-Oct 90*  
pp 135-136

[Article by S. M. Aksamentov, D. I. Matsukov, and V. V. Mitrofanov, Dzershinsk and Novosibirsk]

[Abstract] The problem of gas flow behind a detonation wave was tackled by the method of numerical simulation; the experimental evidence being that the flow is highly nonuniform, indicative of a multifront structure but calculations in the one-dimensional approximation indicating that development of a longitudinal instability results in fluctuations while the leading shock wave and the combustion front oscillate regularly relative to each other. Later experiments have revealed that a secondary detonation wave forms behind the weaker shock wave and accelerates till it reaches the leading shock wavefront and boosts it by a step to an overcompression level. The latest calculations indicate that such a secondary detonation wave is formed by a mechanism associated with the ignition time gradient behind the weaker shock wave, this having been found to occur also in the absence of turbulizers or barriers, other mechanisms being evidently irrelevant here. Figures 1; references 7.

UDC 534.833

### New Method of Calculating Normal Waves in Acoustic Waveguides

917J0028A Moscow AKUSTICHESKIY ZHURNAL  
in Russian Vol 36 No 4, Jul-Aug 90 pp 665-669

[Article by A. M. Zhelvis, Ye. A. Rivelis, and S. Yu. Slavyanov, Leningrad State University]

[Abstract] A new method of calculating the amplitude and the phase of normal sound waves from a point source in a body of water is proposed which treats both amplitude and phase as real quantities in agreement with physical considerations, as quasi-classical quantities in the high-frequency range which facilitates numerical analysis, and as the solution to a system of equations equivalent to the applicable second-order equation. A function  $\psi_n$  which satisfies the equation  $\psi_n + k^2(z)\psi = 0$  ( $z$  - depth coordinate,  $z = 0$  at the surface and  $z = h$  at bottom,  $k$  = square root of  $[\omega/c(z)]^2 - \mu_n^2$ ,  $\omega$  - frequency of wave at source,  $c$  - speed of sound at depth  $z$ ,  $\mu_n$  - eigenvalue) is introduced, accordingly, for both amplitude  $A(z)$  and phase  $\varphi(z)$ . The model of discrete homogeneous horizontal layers where  $\psi^i(z) = A_i \sin(\sum k_j \Delta z_j + k_i(z - z_i + \varphi_i, j = 1, \dots, i - 1))$  is then replaced with a continuous distribution, by replacement of the differences with differentials and the sum with an integral. This leads to a system of two coupled first-order differential equations for functions  $A(z)$  and  $\varphi(z)$  in which the phase appears as the sum of an ordinary Wentzel-Kramers-Brillouin phase  $\tau(z) = \int k(z) dz$  from 0 to  $z$  and an increment due to reflections by inhomogeneities. Assuming that increment  $\varphi(0) = 0$  is at the surface  $z = 0$ , this system of equations can be solved numerically by the Runge-Kutta method or, more efficiently at high frequencies, by the iteration method with the iterated functions  $\varphi_i(z) = \int (k'/2k) \sin(2\tau) dz$  from 0 to  $z$ . The phase velocities of 30 Hz normal waves propagating without refraction through a 0.3 km deep water layer were calculated by this method, assuming a bilinear profile of the speed of sound in water and treating the bed as a half-space filled with a fluid homogeneous material 1.5 times denser than water (speed of sound 1.7 km/s). The phase velocities were not more than 0.4 m/s higher than those obtained by the conventional method of finite differences. The calculation time advantage of the proposed method over the conventional method was, in this case, 1.5 and will increase as the frequency of waves increases. The authors thank A. G. Alenitsyn for performing calculations by the method of finite differences and also for the many consultations. References 8.

UDC 53.01+551.510:534.222.1

### Use of Acoustic Sounding for Determination of Aerosol Parameters

917J0028B Moscow AKUSTICHESKIY ZHURNAL  
in Russian Vol 36 No 4, Jul-Aug 90 pp 712-717

[Article by V. Ye. Nemtsov, Scientific Research Institute of Radio Engineering]

[Abstract] Acoustic sounding of aerosols is considered, the advantages of this method include simplicity of the apparatus and the data processing. It is particularly suitable for objects within close range and facilitates determination of not only the characteristic dimensions of aerosol particles, but also their concentration and size distribution. The method is based on the theory of sound propagation through an air-vapor mixture containing a polydisperse aerosol in the form of water droplets. It takes into account the three influencing dissipative processes, namely evaporation and condensation of water, heat transfer from water droplets to air, and friction between them. In the case of low-frequency sound, all these processes may be regarded as quasi-steady ones and only the Stokes component of the droplet-air interaction force needs to be considered. When the average dimension of droplets is much larger than the mean free path of molecules in air, then condensation of water occurs by diffusion and this process, too, may be regarded as a quasi-steady one. When the specific volume of the liquid phase  $\alpha = Vn < 1$  ( $V$  - average volume of droplet,  $n$  - volume concentration of droplets), then  $\alpha \rho_w < \rho$  as well as  $\rho_v \ll \rho$  ( $\rho, \rho_w, \rho_v$  - density of air, water, and vapor). The closed system of eight equations which describes acoustic sounding under these conditions contains two equations of motion (one for spherical droplets and one for the air-vapor mixture), two equations of continuity (one for air and one for vapor), two linearized equations of energy conservation (one for droplets and one for the air-vapor mixture), one equation of droplet growth, and one equation of state for the air-vapor mixture regarded as a mixture of ideal gases. From this system of equations is derived a dispersion law relating the wave number  $k$  and  $\omega/c_s$  ( $\omega$  - frequency of sound,  $c_s$  - adiabatic velocity of sound in the air-vapor mixture as  $\omega \rightarrow \infty$ ). From this equation, expressions are obtained for the decrement of phase velocity  $(kc_s / \omega) - 1$  and for the attenuation of sound  $\text{Im } k$ . In the range of sound frequencies much higher than the frequencies of droplet velocity and temperature relaxation, both depend not only on these two relaxation frequencies but also on the thermal diffusivity of air and the ambient temperature. In the range of low sound frequencies their dependence on the frequency of sound is parabolic, both also depending on the specific heat of water under constant pressure as well as on the two relaxation frequencies and the ambient temperature. From the areas under curves describing these relations, one can determine the droplet size distribution function  $f(r)dr$  (number of droplets with radii from  $r$  to  $dr$  in unit volume of air-vapor mixture), by equating the integrals of  $(f/r)dr, (f/r^3)dr, r^2 f dr, r^7 f dr$  from 0 to  $\infty$  with their experimentally obtained values. References 16.

UDC 624.07:534.1

### Solitary Wave in Thin Uniformly Curvilinear Beam

917J0028C Moscow AKUSTICHESKIY ZHURNAL  
in Russian Vol 36 No 4, Jul-Aug 90 pp 730-732

[Article by S. A. Rybak and Yu. I. Skrynnikov, Institute of Acoustics imeni N. N. Andreyev, USSR Academy of Sciences]

[Abstract] Propagation of nonlinear elastic waves through thin and uniformly curvilinear beams is considered. Steady-state solutions to the nonlinear equation for a longitudinal strain wave in a straight beam is obtained as a consequence of balance between quadratic hydrodynamic nonlinearity and dispersion of the Klein-Gordon kind in the long-wave approximation. Solutions in the form of solitary waves  $u = u(\eta)$  ( $\eta = x - vt$ ,  $v$  - constant velocity of wave),  $u$  being finite for all finite values of  $\eta$  and vanishing together with its derivative  $\delta u/\delta \eta$  as  $\eta \rightarrow \infty$ , are sought for a beam of circular cross-section. They are obtained by a single integration in a form readily interpreted in terms of analogy to energy and momentum conservation during motion of a particle through a potential field. A potential well forms when and only when the solitary wave is slower than longitudinal strain wave. The profile of such a solitary wave is a symmetric bell curve, both its amplitude and width depending on the wave velocity. In this case, unlike in the case of a KdV soliton, its amplitude is proportional to the width squared. The authors thank Yu. A. Stepanyants for discussion. Figures 2; references 6.

UDC 534.532:517.9

#### Fast Algorithm of Eigenvalue Calculation for Absorbing Multilayer Waveguide

917J0029A Moscow AKUSTICHESKIY ZHURNAL  
in Russian Vol 36 No 6, Nov-Dec 90 pp 965-972

[Article by G. V. Alekseyev and Ye. G. Komarov, Institute of Applied Mathematics, Far Eastern Department, USSR Academy of Sciences]

[Abstract] A fast and efficient accurate algorithm is constructed for numerically evaluating eigenvalues and eigenfunctions needed for solving the singular spectrum problem of ocean acoustics, namely, calculating the acoustic fields in sound absorbing multilayer waveguides. The problem is formulated as a wave equation with a set of boundary conditions at the surface and at the bottom of each successive layer. The problem is solved in three stages: 1) discretization into finite differences, 2) reformulation as a matrix equation  $Ay = \lambda y$  where  $A$  is a tri-diagonal asymmetric nonhermitian matrix and calculating its eigenvalues by the QL-algorithm, and 3) refinement of the obtained eigenvalues by Richardson extrapolation. Inasmuch as the QL-algorithm yields eigenvalues in an arbitrary order, while in problems of ocean acoustics they need to be numbered in the order of decreasing real parts  $\text{Re } \lambda$ , this algorithm is modified so that the first eigenvalue it yields will be the one with the largest real part. The complete algorithm is tested on two semi-infinitely large sound absorbing oceanic waveguide, a triple-layer waveguide and a Pekeris double-layer waveguide with sound absorption in the lowest layer only. Calculations have been made on a Standard System 1061 computer. Figures 1; tables 4; references 21.

UDC 621.373.826:535.36

#### Explosive Boiling and Generation of Shock Waves in Biotissue During Ablation by CO<sub>2</sub> Laser Pulses

917J0029B Moscow AKUSTICHESKIY ZHURNAL  
in Russian Vol 36 No 6, Nov-Dec 90 pp 1016-1020

[Article by A. K. Dmitriyev and N. P. Furzikov, Scientific Research Center for Technological Lasers, USSR Academy of Sciences]

[Abstract] An experimental study of biotissue ablation by pulsed CO<sub>2</sub> laser radiation was made, specimens of artery wall tissue were treated with normally incident 9.26  $\mu\text{m}$  radiation in pulses of 205 - 215 mJ energy and 2  $\mu\text{s}$  duration. The radiation was focused on a spot having an area of 0.13 - 0.15  $\text{cm}^2$ . The space above the tissue specimen was swept vertically by the beam of a continuous-wave He-Ne laser parallel to the tissue surface, with the laser in fixed position and the specimen moved up or down. The supersonic frontal velocity of scattered particles of tissue breakdown products was measured by the time-of-flight method and changes in their optical density were detected by an FD-10 GA photodiode, its output signals being sent through a preamplifier to an S8-12 memory oscillograph for recording the optical density as a function of time. Also the maximum mean temperature of the tissue wall and the maximum mean pressure on it were measured. On the basis of the readings, the time delays from incidence of a laser pulse to the start and to the peak of the photodiode signal were determined, the delays of both becoming longer as the distance of the probing He-Ne laser beam from the tissue surface increased. The data indicate that both the maximum concentration and the frontal velocity of tissue breakdown particles decrease with increasing distance from the tissue surface. An analysis of the data in accordance with the theory of shock waves in gaseous media, indicates an appreciable superheating of tissue above the boiling point of the unevenly distributed tissue water. Inasmuch as surface evaporation is negligible, owing to the finite thermal conductivity of tissue, explosive bulk boiling of the tissue water eventually occurs wherever the local temperature becomes sufficiently high (575 - 592 K) and the mean life of superheated water correspondingly too short. As a result, tissue fibers are destroyed under rising internal pressure, this ablation process begins as the threshold is reached. Figures 3; references 16.

UDC 534.22:539.3

#### Propagation of Undistorted Compression Shock Through Nonlinear Standard Viscoelastic Medium

917J0029C Moscow AKUSTICHESKIY ZHURNAL  
in Russian Vol 36 No 6, Nov-Dec 90 pp 1083-1087

[Article by A. S. Stulov, Institute of Cybernetics, ESSR Academy of Sciences]

[Abstract] Propagation of an acoustic compression shock through a nonlinear standard viscoelastic without distortion is analyzed. A point of departure considered is a one-dimensional longitudinal wave whose parameters are functions of both the Lagrange  $x$ -coordinate and time  $t$  in an initially homogeneous medium with an elastic after-effect constituting a first-order nonlinearity. The wave process is described by an integral equation of the second kind with a creep kernel  $K(t - \tau)$ . The solution to this equation is sought in the form of a compression shock  $U(x,t) = H(\xi)\Psi(\xi)$  propagating at a constant velocity  $v$  in the positive direction, where  $H(\xi)$  is the Heaviside function and  $\Psi(\xi)$  is a smooth function of  $\xi = (t - x/v) / 2\tau_0$ . The relation between breaking stress and wavefront velocity is obtained from the law of momentum conservation. The condition for discontinuity at the

wavefront is obtained from the kinematic identity  $[du/dt] = -v[du/dx]$  ( $u$  - longitudinal displacement). For a standard viscoelastic medium with kernel  $K(t) = (\epsilon/\tau_0)e^{-t/\tau_0}$  ( $\epsilon, \tau_0$  - after-effect parameters of the medium) this equation of state (wave process) is solved by expansion into an infinite series of  $n$  decaying exponential terms with gamma-function coefficients and  $-np\xi$  exponents so that the problem reduces to an algebraic one. Two solutions are obtained, for  $1 \leq p(0) \approx 2.3833$  (root of the equation  $p(0) = 2(1 + 2^{-p(0)})$ ) and for  $p \gg 2$  respectively. These solutions yield a dependence of the shock velocity on  $p$  which indicates that "slow" and "fast" compression shocks can exist in such a nonlinear medium, propagating at velocities respectively lower and higher than the speed of sound in a linear medium. Figures 1; references 4.

UDC 06;12

**Gas-Sensitive Effects in Structures Based on Semiconductor Oxide Systems  $V_2O_5$ - $SnO_2$** *917J0003C Leningrad ZHURNAL TEKHNIЧЕСКОY FIZIKI in Russian Vol 60 No 8, Aug 90 pp 188-190*

[Article by A. S. Tonkoshkur and I. M. Chernenko, Denepetrovsk Institute of Chemical Technology imeni F. E. Dzerzhinsky]

[Abstract] Results are presented from studies of electrical properties, including their variation with the surrounding gas environment, in symmetrical metal-semiconductor-metal structures based on the  $V_2O_5$ - $SnO_2$  oxide system prepared by cooling from the melt. The structures were produced by cathode sputtering of platinum on the surface of samples up to 1 mm thick of  $xV_2O_5 - (1 - x)SnO_2$ , where  $x$  is between 60 and 90 mol.%. It was found that the dc and ac resistance of the specimens depended on the gas environment. The results are physically interpreted by assuming the existence of intercrystalline potential barriers through which the electrical current must flow. Figures 3; references 6: Russian.

**Optical Properties of New Ferroelastic Materials  $[NH_2(C_2H_5)_2]_2 MCl_4$  ( $M = Cu, Co$ )***917J0004A Leningrad PISMA V ZHURNAL TEKHNIЧЕСКОY FIZIKI in Russian Vol 16 No 15, 12 Aug 90 pp 23-26*

[Article by O. G. Blokh, M. I. Bublik, I. I. Polovinko, O. M. Olkhova, S. A. Sveleba, and T. M. Sosnovskiy, Lvov State University imeni I. Franko]

[Abstract] Light absorption spectra of  $[NH_2(C_2H_5)_2]_2 CuCl_4$  and  $[NH_2(C_2H_5)_2]_2 CoCl_4$  crystals were measured over the 293 - 344 K temperature range covering phase transitions in each. Crystals for this study were grown from an aqueous solution of stoichiometric salt mixtures  $NH_2(C_2H_5)_2Cl$  + either  $CuCl_2$  or  $CoCl_2$  by slow evaporation at room temperature. Ferroelectric domains along the c-cut at room temperature and a phase transition of the second kind at 333 K were discovered in the cobalt salt crystals, those domains being easily re-orientable by external mechanical stresses. A phase transition of the first kind at 327 K with an attendant color change to yellow was observed in the copper salt crystals, such a phase transition having been reported earlier at 330 K, but no domain structure was found in these crystals at any temperature below or above that transition point. The absorption spectra of the cobalt salt crystals contain three peaks, a high one with the maximum at the 595 nm wavelength and two successively lower ones with the maxima at 524 nm and 442 nm wavelengths, followed after a deep dip by another higher peak in the ultraviolet

range. The absorption spectra of the copper salt crystals contain two peaks, a high one with the maximum at a wavelength shorter than 500 nm and a lower one at the 595 nm wavelength, with a deep dip between them. The absorption coefficient was, in both cases, to increase from a low value at temperatures below the transition point to a high value at temperatures above the transition point, as indicated by measurements made on the cobalt salt crystals in 400 nm light and on the copper salt crystals in 500 nm light. Figures 2; references 6.

**Optical Properties of the New Ferroelastics  $[NH_2(C_2H_5)_2]_2 CuCl_4$  and  $[NH_2(C_2H_5)_2]_2 CoCl_4$** *917J0011A Leningrad PISMA V ZHURNAL TEKHNIЧЕСКОY FIZIKI in Russian Vol 16 No 15, 12 Aug 90, pp 23-26*

[Article by O. G. Blokh, M. I. Bublik, I. I. Polovinko, O. M. Olkhova, S. A. Sveleba and T. M. Sosnovskiy, Lvov State University imeni I. Franko]

[Abstract] Measurements were made for the first time of the optical absorption spectrum and the temperature dependence of the absorption coefficient at, respectively, 400 and 500 nm of  $[NH_2(C_2H_5)_2]_2 CuCl_4$  and  $[NH_2(C_2H_5)_2]_2 CoCl_4$  crystals at 293 and 344 K. The results indicate a second-order phase transition at 333 K in the  $[NH_2(C_2H_5)_2]_2 CuCl_4$ . A  $160\text{ cm}^{-1}$  change in the crystal field seems to be the reason for a dramatic shift toward lower frequencies in the fundamental absorption edge in  $[NH_2(C_2H_5)_2]_2 CoCl_4$ . Its temperature dependence indicates a first-order phase transition at 333 K. References 6: 1 Russian, 5 Western; figures 2.

**Use of Honeycomb Structures and Polycrystalline Diamond Films in Anodes for Soft X-Ray Sources***917J0011B Leningrad PISMA V ZHURNAL TEKHNIЧЕСКОY FIZIKI in Russian Vol 16 No 15, 12 Aug 90, pp 64-69*

[Article by A. M. Prokhovor, I. N. Sisakin and V. Yu. Khomich, General Physics Institute of the USSR Academy of Sciences, Moscow]

[Abstract] A high-resistance anode and cooling system for use in soft x-ray lithography is proposed. An electron beam incident on the truncated-cone anode excites the characteristic 44.7 angstrom  $K_{\alpha}$  line of carbon in the polycrystalline diamond film outer layer of the copper anode. The heat evolved is carried off by distilled water coolant forced through the underlying honeycomb copper structure layer under 10 atm pressure at a flow-rate of 2 l/min. In tests on a prototype, the anode was found to withstand specific thermal fluxes of about 3 kW/cm<sup>2</sup>, twice that of other designs. References 7: 4 Russian, 3 Western (in Russian translation); figures 1.

### Half-Quantum Vortices in Superfluid $^3\text{He-B}$

917J0015C Moscow PISMA V ZHURNAL  
EKSPERIMENTALNOY I TEORETICHESKOY  
FIZIKI in Russian Vol 52 No 6, 25 Sep 90 pp 972-976

[Article by G. Ye. Volovik, Institute of Theoretical Physics  
imeni L. D. Landau, USSR Academy of Sciences]

[Abstract] Recent nuclear-magnetic-resonance experiments confirmed what numerical analysis and calculations have predicted, namely the existence of two kinds of vortices in superfluid  $^3\text{He-B}$  separated by the  $B \rightarrow A$  phase transition line in the  $H-T$  plane ( $H$  - intensity of external magnetic field,  $T$  - temperature); an axisymmetric one containing some  $^3\text{He-B}$  phase in its eye and a nonaxisymmetric one. The latter, existing not only in the stable  $B$ -phase at temperatures below the  $B \rightarrow A$  phase transition line but also in the superheated and thus metastable  $B$ -phase between the  $B \rightarrow A$  transition line and the  $A \rightarrow P$  phase transition line, has been interpreted as being a pair of vortices with half a circulation quantum each. It is now demonstrated that as the magnetic field intensity, under low pressure, is raised at some temperature below critical, these two half-quantum vortices become sufficiently isolated from each other so that the distance between them may reach the dimension of the vortex cell rather than only the dimension of the vortex eye of the order of the coherence length. Under low pressure, the strong-link effects are negligible and the energy of the  $A$ -phase is comparable with the energy of the always metastable planar ( $P$ ) phase, of particular concern is the asymmetric vortex in the metastable  $B$ -phase existing along with the stable  $A$ -phase and the metastable  $P$ -phase under low pressure in a strong magnetic field. While originating at the critical  $T_c$  temperature point in a zero magnetic field, where the  $B \rightarrow A$  transition line originates, the same magnetic field intensity corresponds to a higher temperature on the  $A \rightarrow P$  transition line than on the  $B \rightarrow A$  transition line and thus, the same temperature corresponds to a higher magnetic field intensity on the  $A \rightarrow P$  transition line than on the  $B \rightarrow A$  transition line. One point through which the  $A \rightarrow P$  transition line passes is the  $B$ - $A$ - $P$  triple point  $T_0 - H_0$  ( $T_0$  in the vicinity of  $0.8 T_c$  and  $H_0$  about 2 kG), the transition from metastable  $B$ -phase to metastable  $P$ -phase being of the first kind at temperatures below that point (strong magnetic field) and of the second kind above that point (weak magnetic field). The structure of such an asymmetric vortex in the  $B$ -phase near the  $B \rightarrow P$  phase transition of the second kind is considered and the energy dependence of the distance between its half-quantum components is analyzed in accordance with the Bardeen-Cooper-Schrieffer theory, deviations from which are negligible in the given case. Dissociation of a compound object consisting of a vortex ( $N = 1$ ) and a disclination ( $N, p) = (1, 1)$  into one consisting of two identical half-vortices with half-charges ( $N, p) = (1/2, 1/2)$  is shown, the domain wall having been broken in the process and two half-vortices with opposite charges ( $N, p) = (1/2, -1/2)$ , ( $N, p) = (-1/2, 1/2)$  then existing in the intermediate state. Their motion results in separate

formation of a disclination ( $N, p) = (0, 1)$  and a vortex ( $N, p) = (1, 0)$ , the latter consisting of a pair of half-vortices with charges ( $N, p) = (1/2, 1/2)$  and ( $N, p) = (1/2, -1/2)$  respectively. The author thanks J. P. Pekola and M. Krusius for valuable discussions. Figures 3; references 13.

### Structure of Surface Layer in Superfluid $^3\text{He-B}$

917J0015D Moscow PISMA V ZHURNAL  
EKSPERIMENTALNOY I TEORETICHESKOY  
FIZIKI in Russian Vol 52 No 6, 25 Sep 90 pp 976-979

[Article by G. Ye. Volovik, Institute of Theoretical Physics  
imeni L. D. Landau, USSR Academy of Sciences]

[Abstract] The problem of determining the structure of the superfluid  $^3\text{He-B}$  boundary layer at the container wall in terms of the order parameter is considered, its determination having been made so far by numerical analysis of the Ginzburg-Landau equations for a multi-component order parameter or of quasi-classical equations for Green's functions and analytically, only for the  $B$ -phase near the  $B \rightarrow A$  phase transitions with a distinct interphase boundary. Analytical determination of the four most important surface layer structures ( $P^{1,2}$  and  $A^{1,2}$ ), is shown to be possible within certain ranges of temperature  $T$ , pressure  $P$ , and magnetic field intensity  $H$ . Their existence is due to the fact that the  $B$ -phase does not wet the container wall and an intermediate layer of another phase must therefore be interceding. Each of these structures, a layer of the planar ( $P$ ) phase or of the  $A$ -phase, accordingly separates the boundary from the nearby particular interphase boundary. The difference between ( $P, A^1$ ) and ( $P, A^2$ ) structures is that the (1) structures have a nonuniformly oriented orbital vector, its orientation varying from normal at the container wall to tangential at the interphase boundary. Each structure, moreover, has a symmetry of a different class:  $P^1$  - class 17,  $A^1$  - class 11,  $P^2$  - class 8,  $A^2$  - class 3. They can therefore exist within ranges of  $T, P, H$  beyond their analytical determinability. Analytical determination of the  $A^{1,2}$  structures involves the dependence of their energy on the distance from the  $A$ - $B$  boundary to the container wall, the dependence being exponential for the  $A^1$  structure and a power-law dependence for the  $A^2$  structure. Analytical determination of the  $P^{1,2}$  structures needs to take into account that formation of a well developed  $P$ -phase requires that the  $B \rightarrow P$  phase transition of the first kind, in a strong magnetic field ( $H \gg 2$  mT) under low pressure, be very close to the  $B \rightarrow A$  phase transition. The author thanks M. Krusius, V. P. Mineyev, J. P. Pekola, and M. M. Salomaa for valuable discussions. Figures 1; references 14.

### Effect of Dissipation on Structure of Stationary Wave Turbulence Spectrum

917J0033A Moscow ZHURNAL  
EKSPERIMENTALNOY I TEORETICHESKOY  
FIZIKI in Russian Vol 98 No 6(12), Dec 90  
pp 1931-1940

[Article by I. V. Ryzhenkova and G. Ye. Falkovich,  
Institute of Automation and Electrometry, Siberian  
Department, USSR Academy of Sciences]

[Abstract] The stationary spectrum of wave turbulence is analyzed for the effect of dissipation distributed in the wave number  $k$ -space. A weak wave turbulence is considered with a long inertia interval between regions of wave generation and attenuation, and with a dispersion law of the decay kind involving three-wave processes. The collision integral satisfies both energy and momentum conservation laws, interaction of waves and the ambient medium described by a function which is positive in the source region and negative in the drain region. The fundamental equation of kinetics yields the condition for existence of a stationary nonequilibrium dissipation distribution, which is the presence of an energy source in the region of large wave numbers  $k \ll k_m$  ( $m$  - homogeneity index), and also the form of the wave attenuation function. The theory is applied to a model system with three spherical harmonics, corresponding to three points in the frequency  $\omega$ -space. Next, the distorting effect of a remote dissipative region on the Kolmogorov distribution within the inertia space is determined. The results of theoretical analysis have been validated by numerical analysis of wave turbulence with dissipation involving capillary waves in deep water, gravitational-capillary waves in shallow water, and three-dimensional sound waves with positive dispersion. As a special case, the behavior of the stationary wave turbulence spectrum within a region of strong dissipation with wave numbers  $k \leq k_m$  is considered. Figures 4; references 10.

#### Generation, Annihilation, and Soliton-Like Passage of Vertical Bloch Line Clusters in Domain Wall of Ferromagnet

917J0033B Moscow ZHURNAL  
EKSPERIMENTALNOY I TEORETICHESKOY  
FIZIKI in Russian Vol 98 No 6(12), Dec 90  
pp 2011-2017

[Article by Ye. Ye. Kotova and V. M. Chetverikov,  
Moscow Institute of Electronic Machine Design]

[Abstract] The behavior of vertical Bloch lines in a film of a uniaxial ferromagnetic material with cylindrical magnetic domains is analyzed, such Bloch lines are known to form clusters between oppositely polarized subdomains. Analysis of the dynamics of these clusters, including their soliton-like passage through one another as well as formation and annihilation of new ones in the process, is based on Slonchewski's equations. The complete equations have been reduced by averaging over the film thickness, assuming a negligible twist of the domain wall, but the non-local magnetic field component  $H_x^{cf}$  along the domain wall has been retained so as to correctly account for magnetostatic interaction of vertical Bloch lines within a cluster as well as between clusters.

The system of these two differential equations, with an improper integral representing the  $H_x^{cf}(x,t)$  component in the second equation, has been solved numerically by the method of finite differences according to an implicit scheme and matrix reduction. This system of equations is not a completely integrable one but, depending on the relations between its parameters, is found to have soliton-like solutions or solutions corresponding to generation and annihilation of solitons. The results of numerical calculations agree quite well with the results of physical experiments. The authors thank M. V. Chetkin for discussing this agreement. Figures 4; references 10.

#### Effect of Crystal Structure Characteristics on Magnetic Properties of $Nd_2CuO_4$

917J0033C Moscow ZHURNAL  
EKSPERIMENTALNOY I TEORETICHESKOY  
FIZIKI in Russian Vol 98 No 6(12), Dec 90  
pp 2098-2109

[Article by V. A. Blinkin, I. M. Vitebskiy, O. D. Kolotiy,  
N. M. Lavrinenko, V.P. Seminozhenko, and V.L. Sobolev,  
Scientific-Industrial Association "Monokristallreaktiv"  
(Single-Crystal Reagent)]

[Abstract] Magnetic ordering of  $Nd_2CuO_4$ , basic compound in a new class of high- $T_c$  superconductor materials with a b.c.c. tetragonal lattice in the  $I4/mmm$  symmetry group, is analyzed by application of standard group theory and considering only uniform states ( $k = 0$ ) of the magnetic subsystem. Symmetry of spin-spin interactions yields four planar noncollinear-exchange magnetic structures and two equivalent collinear antiferromagnetic ones. In addition to a structural phase transition due to structural distortions, the analysis thus reveals a set of magnetic phase transitions. Uniform vibrations of the spin system are examined, considering that at moderate temperatures the Nd magnetic subsystem only renormalizes the parameters in the spin Hamiltonian of the Cu magnetic subsystem. In this case four modes of antiferromagnetic resonance, one normal exchange mode and three normal acoustic ones, occur in each of the four exchange-noncollinear phases. Inasmuch as magnetic ordering can appreciably alter the macroscopic, and thus tensorial properties of a crystal, various effects characteristic of magnetically ordered crystals known to result from spin-lattice interaction, the dominant exchange part of this interaction along with spontaneous distortions of the crystal structure at temperatures below critical is shown to be responsible for the linear magnetoelectric effect in noncollinear-exchange structures and also in equivalent collinear ones. The authors thank A. S. Borovik-Romanov, V. V. Yerenko, V. I. Ozhogin, and L. A. Prozorova for support and helpful discussions. Figures 6; tables 5; references 9.

UDC 01:10

**Collective Induced Radiation of Spatially Limited Groups of Electron Oscillators: Channeling and Superradiant Radiation**

917J0003A Leningrad ZHURNAL TEKHNICHESKOY FIZIKI in Russian Vol 60 No 8, Aug 90 pp 40-53

[Article by N. S. Ginzburg and A. S. Sergeev, Institute of Applied Physics, USSR Academy of Sciences, Gorkiy]

[Abstract] A study is made of two characteristic types of problems: spatial amplification of monochromatic quasi-optical electromagnetic beams in an electron waveguide consisting of a layer of particles oscillating in a periodic magnetic field, and the problem of superradiant time relaxation of a layer of cyclotron oscillators forming an electronic resonator in a medium with an index of refraction which approaches zero, such as a plasma, a waveguide near the cutoff frequency. Both the linear and the nonlinear stages of the interaction are discussed and it is demonstrated that the problems are similar if the space variable is replaced by a time variable. It is shown that, in the linear stage, amplification and channeling of radiation by the electron beam occurs; in the nonlinear stage, the diffraction effects lead to expansion of the wavebeam and radiation of a large portion of the electromagnetic energy generated by the electron beam into the surrounding space. A steady soliton-like state of the wavebeam is subsequently set up, capturing electrons in the flow and channeling them by total internal reflection. An analogy is noted between radiation with channeling and the superradiant time relaxation of a layer of cyclotron oscillators in a medium with a near-zero index of refraction. Figures 9; references 28: 22 Russian, 6 Western.

UDC 07

**Aberration Thermocapillary Transformation of Laser Beams**

917J0003B Leningrad ZHURNAL TEKHNICHESKOY FIZIKI in Russian Vol 60 No 8, Aug 90 pp 103-108

[Article by S. A. Viznyuk, S. F. Rastopov, and A. T. Sukhodol'skiy, Institute of General Physics, USSR Academy of Sciences, Moscow]

[Abstract] Results are presented from experiments and calculations investigating the aberration nature of the conversion of Gaussian laser beams on a thin layer of a viscous fluid heated by the laser beam. A numerical calculation of the aberration picture is undertaken for thermocapillary conversion in the approximation of geometric optics, and by calculating the Kirkhoff integral based on the measured profile of the thermocapillary lens. Studies are performed with argon and CO<sub>2</sub> lasers. As the thickness of the layer is increased additional band points appear on the profile as a result of the increasing significance of convection as the thickness increases and

its competition with Marangoni forces on the surface. As the diameter of the beam increases, the aberration picture takes on a ring shape with sharp inner and outer edges and a drop in intensity in the center. Figures 3; references 9: 4 Russian, 5 Western.

**Femtosecond Relaxation of Excited Carriers in CdSe(x)S(1-x) Microcrystals Glass Matrix After High-Intensity Excitation**

917J0006B Moscow PISMA V ZHURNAL EKSPERIMENTALNOY I TEORETICHESKOY FIZIKI in Russian Vol 52 No 4, 25 Aug 90 pp 851-854

[Article by Yu. Ye. Lozovik, Yu. A. Matveyets, A. G. Stepanov, V. M. Farztdinov, S. V. Chekalin, and A. P. Yartsev, Institute of Spectroscopy, USSR Academy of Sciences]

[Abstract] Relaxation of excited carriers in glass containing CdSe<sub>x</sub>S<sub>1-x</sub> microcrystals was studied in an experiment, industrial RC-8 Schott filters of such a glass with a high concentration of these microcrystals, excited with pulses of femtosecond duration, and an intensity up to the breakdown threshold. After excitation of a 400 μm thick glass specimen with a 300 fs pulse of 612 nm radiation, 200 meV above the bottom level of the conduction band, the affected region was probed with a femtosecond pulse of a wideband spectral continuum with lagging excitation pulse. The intensity of excitation was varied over the 0.01 - 10 TW/cm<sup>3</sup> range by means of neutral light filters and by sharper focusing. The intensity of the probing pulse did not exceed 1 GW/cm<sup>3</sup>. The absorption dynamics and spectra of the specimen before and after excitation were recorded in a multichannel optical analyzer covering the 600 - 720 nm range of wavelength, after a computer had been hooked on for calculation of the difference spectra as the delay of the probing pulse was varied. On the basis of these data was determined the dependence of the optical density of the specimen on the intensity of the excitation pulse, the glass clearing almost completely as the excitation intensity was raised to 1 TW/cm<sup>3</sup> and then beginning to absorb radiation until breaking down as the excitation intensity was raised to 10 TW/cm<sup>3</sup>. Both calculated and measured difference spectra indicate a carrier relaxation time not longer than 30 fs after an excitation of 0.1 TW/cm<sup>3</sup>, while theoretical estimates yield not longer than 0.1 fs relaxation to the bottom of the conduction band and subsequent 500 ps recombination time. They reveal a wider bleaching range with the peak shifted toward shorter waves, as the bands become filled with carriers. While two-photon processes are evidently negligible after excitation with an intensity lower than 0.1 TW/cm<sup>3</sup>, recombination seems to occur by the Auger mechanism. The authors thank V. S. Letokhov for valuable discussions. Figures 2; references 7.

UDC 621.373.826:533.9

**High-Speed X-Ray Electron-Optical Diagnostics of a Laser Plasma***917J0009A Moscow KVANTOVAYA ELEKTRONIKA in Russian Vol 17 No 9, Sep 90 pp 1101-1134*

[Article by V. K. Chevokin, USSR Academy of Sciences General Physics Institute, Moscow]

[Abstract] X-ray electron-optical cameras for diagnosis of soft X-ray radiation from laser plasmas are reviewed. The technical and general characteristics of a variety of electron-optical transducers and cameras based on them are given, including: the American RCA C73435 developed at Livermore Labs, the Soviet UMI-93Sr and UMI-92 developed jointly by FIAN and VNIIOFI, the British Headland Photonics X-CHRON400 and X-CHRON540, the French TSN-503X, TSN-504X and TSN-505X developed at the Commissariat de Energie Atomique, the Los Alamos Pico-X, the C1936 and C1102X cameras built by Hamamatsu (Japan), and the Soviet Almaz-R camera. Results of dynamic tests of these devices and procedures for their use in laser plasma diagnostics are presented. Registering radiation from laser plasmas using fast plastic scintillators with subnanosecond time resolution is discussed. The spectral dependence of quantum yield and volta-ampere characteristics of various photocathodes used in X-ray electron-optical transducers are determined. There is discussion of X-ray electron-optical diagnostics of laser plasmas formed by pico- and femtosecond pulses. A brief analysis is made of recent advances reported at the 1988 18th International Congress on High-Speed Photography and Photonics in Xi'an, China. References 148: 75 Russian, 73 Western; figures 31; tables 7.

UDC 621.373.826.038.825.2

**A Free-Running and Q-Switched Erbium Mini-Laser***917J0009B Moscow KVANTOVAYA ELEKTRONIKA in Russian Vol 17 No 9, Sep 90 pp 1156-1157*

[Article by I. L. Vorobyev, V. P. Gapontsev, A. K. Gromov, A. A. Izyneyev, A. M. Onishchenko and P. I. Sadovskiy, USSR Academy of Sciences Radio Technology and Electronics Institute, Moscow]

[Abstract] The authors have developed a laser based on chromium-ytterbium-erbium LGS-Kh glass. It has a differential efficiency of 3.5 percent at 22 J pumping threshold, and a new high for erbium lasers, 2.5 percent absolute efficiency at 100 J pumping under free-running operation. Under Q-switched operation, maximum efficiency of 0.27 percent is attained at 37 J for single pulses of up to 100 mJ. References 2: 1 Russian, 1 Western; figures 3.

UDC 621.373.826

**The Effect of Inter-Cavity Medium on Laser Mode Gain in a Wideband Laser***917J0009C Moscow KVANTOVAYA ELEKTRONIKA in Russian Vol 17 No 9, Sep 90 pp 1158-1162*

[Article by S. A. Kovalenko and S. P. Semin, Physical-Technical and Radio-Technical Measurements SRI (A-U), Mendeleyevo, Moscow oblast]

[Abstract] Starting from balance equations for a slowly varying multimode broadband laser, it is shown analytically that taking into account amplitude beating of the various modes gives an increased gain coefficient. Physically, this beating is caused by spatial inhomogeneities in the intracavity medium and their focussing properties. Focusing action by intracavity active medium shifts the position of the laser emission band. The self-focusing effect in an absorbing medium results in increased gain, but this increase is slight and so it cannot be the mechanism behind spectrum condensation and absorption lineshape distortion. References 15: 8 Russian, 7 Western; figures 1.

UDC 621.373.826

**Efficient Parametric Light Beam Amplification. I. Optimization of Parametrically-Amplified Interacting Wave Profiles***917J0009D Moscow KVANTOVAYA ELEKTRONIKA in Russian Vol 17 No 9, Sep 90 pp 1192-1196*

[Article by I. A. Begishev, A. A. Gulamov, Ye. A. Yerofeyev, E. A. Ibragimov, Sh. R. Kamalov, T. Usmanov and A. D. Khadzhayev, Uzbek SSR Academy of Sciences Electronics Institute imeni A. A. Arifov, Tashkent]

[Abstract] A theoretical model is developed showing that the efficiency of pumping energy conversion in lasing is very sensitive to the shape (Gaussian, hyper-Gaussian) of spatial-temporal modulation of the seed signal and pumping signal. One hundred percent conversion is possible when the processes of energy transfer between the output wave and the pumping wave,  $\omega_1 + \omega_2$  goes to  $\omega_3$  and  $\omega_3$  goes to  $\omega_1 + \omega_2$ , are mutually inverse, i.e., the wave profiles are conformal; in one experiment where this condition was met the efficiency exceeded 95 percent. Profile contrast, i.e., the ratio of maximum intensity to intensity in the center, and length of the nonlinear medium are optimized for the seed signal. Limiting values of the conversion factor as a function of seed and pump energies and the spatial-temporal shape of these pulses are determined. References 9: 7 Russian, 2 Western; figures 6.

UDC 621.373.826.038.823

### **A Dynamic Model of Active Mode Locking in a Gas Laser**

917J0009E Moscow KVANTOVAYA ELEKTRONIKA  
in Russian Vol 17 No 9, Sep 90 pp 1219-1223

[Article by L. A. Melnikov, G. N. Tatarkov, Mechanics and Physics SRI, Saratov State University]

[Abstract] The authors develop an analytical model of active mode locking in gas lasers with inhomogeneously broadened active medium based on a temporal, rather than frequency (mode) description. A numerical experiment based on this model shows that when active mode locking is disrupted in the system, complex quasiperiodic dynamic modes result, becoming more chaotic as the loss modulation depth is decreased. The numerical algorithm, which assumes that small gain in a single pass through the medium, is shown to be inadequate for description of argon ion lasers. The complex multi-hump shape of each single pulse is shown to be governed by the coherent interaction between the pulse and the active medium; the modulator serves only to regulate the pulse overlap conditions of this interaction. References 14: 6 Russian, 8 Western; figures 6.

### **Laser Beams With Screw Dislocations of Wavefront**

917J0022A Moscow PISMA V ZHURNAL  
EKSPERIMENTALNOY I TEORETICHESKOY  
FIZIKI in Russian Vol 52 No 8, 25 Oct 90  
pp 1037-1039

[Article by V. Yu. Bazhenov, M. V. Vasnetsov, and M. S. Soskin, Institute of Physics, UkSSR Academy of Sciences]

[Abstract] An experimental study of a He-Ne laser was made, its purpose being the production and examination of regular coherent light fields with screw dislocations (optical vortices) in the beam. The apparatus consisted of a beam expander and Mach-Zehnder interferometer with a bundle of multimode optical fibers behind an objective lens in one arm. Radiation with a Gaussian mode was focused onto the entrance aperture of one fiber, a pattern of two or three irregularly shaped spots then appearing in the exit aperture of that fiber. A biconcave lens in the reference arm equalized the divergences of interfering partial beams. Rotation of the semi-transparent exit mirror exposed the interference patterns within various regions of the laser beam leaving the fiber waveguide. A usual ring pattern was observed in regions of maximum illuminance, but a dislocation at the center of such a region deformed this pattern into a spiral one with zero illuminance at the center. Wherever interfering partial beams reached the screen at small angles to one another, the interference fringe either split or vanished just as in the case of a dislocation in speckle fields. Dislocations observed in this experiment were of either +1 or -1 order, the numbers of right-hand and

left-hand screw dislocations being equal. In order to observe higher-order dislocations, it was necessary to synthesize amplitude holograms simulating the interference field of a plane wave and a wave with a dislocation of a given order. The fiber bundle and the objective lens were replaced by these holograms as diffraction gratings, for a study of dislocations in higher diffraction orders without using the beam expander. The radiance dip at the center of the laser beam was found to become steeper as the dislocation order became higher. Interference with the reference wave produced a pattern with spiral inclusions, their number being equal to the dislocation order. The authors thank S. G. Odulov and V. V. Shkunov for helpful discussions. Figures 2; references 2.

UDC 621.373.826.038.823

### **On Ultimate Efficiency of Heavy Inert Atom Lasers With d-p Transitions**

917J0043A Moscow KVANTOVAYA ELEKTRONIKA  
in Russian Vol 17 No 12, Dec 90 pp 1537-1538

[Article by B. M. Berkeliyev, V. A. Dolgikh, I. G. Rudoy, A. M. Soroka, Scientific Research Center for Industrial Lasers at the USSR Academy of Sciences, Shatura]

[Abstract] It is shown that the efficiency (KPD) of near infrared (IK) heavy inert atom lasers with *d-p* transitions and ionizing pumping may substantially exceed the "quantum" value. The conditions for attaining the limit of efficiency in argon lasers are discussed. It is shown that the lasing energy decreases substantially at nitrogen pressures of 1 mm Hg, i.e., at its concentration of about 0.02 percent; the conditions are significantly more stringent for the H<sub>2</sub>, CO, CO<sub>2</sub>, and H<sub>2</sub>O impurities. It is also demonstrated that the associative ionization frequency decreases with a decrease in the current density thus necessitating a decrease in the impurity concentration in helium. It may also be necessary to reduce the active medium pressure and/or argon concentration in it in order to lower the argon excimer generation rate. References 10: 9 Russian, 1 Western; figures 1.

UDC 621.373.826:681.3

### **Optical Logic Elements for High-Throughput Optical Processors**

917J0043B Moscow KVANTOVAYA ELEKTRONIKA  
in Russian Vol 17 No 12, Dec 90 pp 1539-1545

[Article by V. B. Fedorov, Joint Computer Center at the USSR Academy of Sciences, Moscow]

[Abstract] Research and development of optical logic elements (OLE) and threshold light amplifiers (PUS) for high-throughput computers, particularly for digital optical processors (OP), are summarized. Today's state of these efforts is analyzed and the outlook for developing OLE and PUS is examined from the viewpoint of

the possibility of designing them on the basis of high-throughput computers. A possible design of an optical processor with a speed of 10 - 100 million mips with two-dimensional arrays of multi-digit binary operands in the pipelining mode is examined in detail. Basic requirements to be imposed on the parameters and characteristics of optical logic elements in such a processor are formulated. It is shown that if existing physical, technological, and engineering problems are overcome, it will be possible to implement OP whose throughput is competitive with that of advanced designs of VLSI circuit processors. References 49: 8 Russian, 41 Western; figures 6.

UDC 621.373.826.038.823

**XeCl Laser Excited by Microwave  
Microsecond-Long Megawatt Pulses of a 3.07  
GHz Industrial Microwave Oscillator**

917J0043C Moscow KVANTOVAYA ELEKTRONIKA  
in Russian Vol 17 No 12, Dec 90 pp 1548-1549

[Article by V. A. Vaulin, V. N. Slinko, S. S. Sulakshin,  
Scientific Research Institute of Nuclear Physics at the  
Tomsk Polytechnic Institute imeni S. M. Kirov]

[Abstract] Stimulated emission on a wavelength of 308 nm was achieved in a Ne-Xe excimer laser excited by microwave pulses at a 3.07 GHz frequency with a duration of 2.8  $\mu$ s and a power of about 0.9 MW using an industrial microwave oscillator. The peak laser radiation power reached 130 W with a pulse duration of 280 ns. In addition to lasing from the skin layer region, laser radiation emitted from the center of the laser tube was also recorded. It is shown that the results of the experiment are preliminary since the optical resonator, the electrodynamic structure parameters of the microwave

pulse injection into the gas and, consequently, the pump power were not being optimized; despite that, the resulting lasing parameters are comparable to those achieved in early efforts to develop a XeCl excimer laser with microwave pumping. Laser radiation was also recorded outside the electromagnetic wave scanning area. References 10: 8 Russian, 2 Western; figures 2.

UDC 681.7.068:535.3

**Vector Solitons in Fiber Optic Waveguide With  
Random Birefringence**

917J0043D Moscow KVANTOVAYA ELEKTRONIKA  
in Russian Vol 17 No 12, Dec 90 pp 1599-1602

[Article by Yu. S. Kivshar, V. V. Konotop, Radio  
Physics and Electronics Institute at the Ukrainian  
Academy of Sciences, Kharkov]

[Abstract] Soliton pulse propagation was examined in single-mode fiber optic waveguides with birefringence; it is shown that it leads to a nonlinear interaction of polarizations as well as differences in their group velocities. It is demonstrated that if the parameter which characterizes the birefringence intensity exceeds the critical value, the soliton decays. Special attention is focused on the case where birefringence is described by a random function. It is also shown that fluctuations of birefringence invariably split vector solitons into individual polarizations whereby the characteristic distance which determines this splitting can be computed analytically. It is asserted that the resulting estimates adequately describe the decay of vector solitons caused by the birefringence parameter fluctuations. The authors are grateful to L. F. Mollenauer, V. N. Serkin, and A. Hasegawa for discussing the results and to C. R. Menyuk for stimulating discussions of the problem formulation. References 17: 2 Russian, 15 Western; figures 1.

UDC 538.9

### Solitons in Atomic Chain Under External Tension

917J0005A Leningrad FIZIKA TVERDOGO TELA  
in Russian Vol 32 No 7, Jul 90 pp 1992-1995

[Article by R. Kh. Sabirov, Moscow State Pedagogical  
Institute imeni V. I. Lenin, Moscow]

[Abstract] Propagation of solitons along an atomic chain with cubic and quartic anharmonicity under external tension is analyzed in the approximation of continuum physics (R.Kh. Sabirov, FIZIKA TVERDOGO TELA Vol 31 No 4, 1989); only those branches of the soliton solution to the equation of motion are considered on which transverse displacement approaches zero as the elongating force decreases to zero. These branches of the solution are analyzed for the dependence of the soliton amplitude and of the soliton velocity, normalized to the velocity of sound, on the magnitude of that force. Numerical analysis and calculations indicate that external tension appreciably influences the behavior of solitons in such a chain, a critical value of the parameter  $b = \alpha\gamma/\beta^2$  ( $\alpha$  - elasticity constant,  $\beta, \gamma$  - anharmonicity constants) being  $3/8$ . An elongating force lowers the amplitudes of both tension and compression solitons, tension solitons remaining the "larger" ones, when  $b \leq 3/8$ . As the elongating force reaches a critical magnitude  $F^*$ , compression solitons cease to exist and tension solitons also cease to exist when  $b = 3/8$ . When  $b > 3/8$ , then the amplitude of tension solitons decreases and the amplitude of compression solitons increases until both amplitudes become equal as the elongating force reaches a critical magnitude  $F_0$ . That critical magnitude depends strongly on the magnitude of  $b$ , the relation approaching an inverse proportion. As the elongating force increases above this critical magnitude, moreover, compression solitons become the "larger" ones. Figures 4; references 1.

UDC 534.222.2:530.1

### Propagation of Solitons Within Phase Transition Range in External Field

917J0005B Leningrad FIZIKA TVERDOGO TELA  
in Russian Vol 32 No 7, Jul 90 pp 2118-2120

[Article by V. I. Serikov and S. V. Voronin, Lipetsk  
Polytechnic Institute]

[Abstract] Propagation of solitons of scalar field ordering within phase transition range is analyzed on the basis of the Ginzburg-Landau equation describing relaxation of such a field in the presence of an external coupled to the order parameter, with the free energy regarded as a functional of both fields in the approximation of a uniform order parameter distribution. In the more general case of a coupled external field with a constant component, as well as an alternating component in the form of a solitary wave, the solution to the appropriately

modified Ginzburg-Landau equation yields the conditions for existence of order parameter solitons. For a purely alternating external field, the equation has four different soliton solutions, all vanishing at the critical phase transition temperature. For a mixed external field, there exist three real solutions when the external field has a constant component of a magnitude smaller than a critical one. Above the critical temperature, there are no soliton solutions for an external field with a constant component of a magnitude much smaller than that critical one. References 4.

UDC 538.69:539.124

### Soliton and Domain Parts of Nonequilibrium Dielectric Permittivity of $\text{Rb}_2\text{ZnCl}_4$

917J0005C Leningrad FIZIKA TVERDOGO TELA  
in Russian Vol 32 No 7, Jul 90 pp 2172-2174

[Article by S. A. Gridnev, S. A. Prasolov, and V. V. Gorbatenko, Voronezh Polytechnic Institute]

[Abstract] It had been established earlier that at least two processes with a characteristic relaxation time are both responsible for a metastable state of the commensurate ferroelectric phase in  $\text{Rb}_2\text{ZnCl}_4$  crystals, namely the pinning of the domain walls which have formed below the noncommensurate-to-commensurate phase transition temperature and change in the concentration of solitons which have not decayed at that temperature. An experimental study was made for the purpose of separating and evaluating the contributions of these two processes to the nonequilibrium part of the dielectric permittivity as well as its equilibrium part. Crystals were grown from a super-saturated aqueous  $\text{Rb}_2\text{ZnCl}_4$  solution by controlled cooling of the latter. Both total dielectric permittivity and total conductance of 0.5 mm thick X-cut  $5 \times 7 \text{ mm}^2$  slices were measured at a frequency of 1592 Hz in an electric field of 0.3 V/cm intensity. The temperature was varied at a rate of about 0.3 K/min or held constant at various points covering the 140 - 200 K range, 197 K being the transition point and the equilibrium part being measured at temperatures below the range of the metastable state. The temperature dependence of the dielectric permittivity and the relaxation characteristics of both processes involved reveal that the metastable state attributable to concurrently active domain wall formation and soliton decay processes exist in a crystal cooled from room temperature to within a 5.3 K temperature range just below the transition point. It is cooled to still lower temperatures inhibiting the domain wall formation process and leaving only the soliton decay process. The equilibrium part of the dielectric permittivity drops from within the narrow 155 - 152.5 K temperature to a smaller magnitude which then remains constant as the temperature is further lowered. This is the same temperature range within which lies the lower limit for existence of the metastable state, and within which the relaxation constant for the soliton decay process decreases from 1000 min to 20 s. The authors thank L. A.

Shuvalov for interest and V. M. Varikash for supplying the crystals. Figures 2; references 2.

### Possible Anomalous Interactions Between Ultracold Neutrons

917J0006A Moscow PISMA V ZHURNAL  
EKSPERIMENTALNOY I TEORETICHESKOY  
FIZIKI in Russian Vol 52 No 4, 25 Aug 90 pp 840-842

[Article by V. A. Artemyev, Institute of Metallurgy imeni A. A. Baykov, USSR Academy of Sciences]

[Abstract] Storing ultracold neutrons by deposition on a planar substrate in a gravitational field is considered, after having been proposed as a method of obtaining 2D-n neutrons in two-dimensional motion with 1.4 peV and 2.45 peV first and second gravitational energy levels. Elastic scattering of such neutrons at the first level with an energy of their relative motion smaller than  $(2.45 - 1.4) = 1.05$  peV so that transition to a higher gravitational level cannot occur is described in terms of the Fermi pseudopotential and by the corresponding wave function. The cross-section for their elastic scattering is calculated on this basis and found to be inversely proportional to the square root of the energy of their relative motion within the range corresponding to significant quantization in a compressing field, while for 3D-n neutrons in three-dimensional motion under conditions of weightlessness, the scattering cross-section remains constant as the energy of their relative motion decreases to zero. As the energy of their relative motion increases, it reaches the range in which transitions of 2D-n neutrons from one gravitational level to another can occur. On a substrate with whiskers in a gravitational field, 1D-n neutrons in free one-dimensional motion along the whiskers can be obtained, their motion in any other direction being forbidden and the gravitational field together with the substrate material thus forming an "ideal" resonator so that the  $c$ -nucleus  $\rightarrow$  nucleus + neutron decay channel becomes either partly or completely suppressed. It is furthermore possible for 1D-n neutrons obtained by dimensional quantization in a substrate channel with a diameter about equal to the limiting wavelength of ultracold neutrons to exist in a bound  $n_2$  state with the molecule  $l = 10$  m long, according to calculations made by the variational method. With ultracold neutrons in a centrifuge, the gravitational field can be boosted enough so that these possibilities may also apply to 0.1 - 10 neV ultracold neutrons. The author thanks Professor M. V. Kazarnovskiy for support and helpful discussions. Figures 2; references 2.

### Interaction of Solitary Waves in System of Born-Infeld Equations

917J0008A Moscow TEORETICHESKAYA I  
MATEMATICHESKAYA FIZIKA in Russian Vol 84  
No 2, Aug 90 pp 181-194

[Article by O. F. Menyshikh, Kuybyshev Institute of Aviation]

[Abstract] The system of quasi-linear Born-Infeld equations describing an extremal surface in an  $(n + 2)$  dimensional pseudo-euclidean space with the  $(dS)^2 = (dt)^2 - (dx)^2 - \sum (dU_i)^2$  over  $i$  from 1 to  $n$  when such a surface is given in the form of  $U_i = U_i(x, t)$  ( $i = [1, n]$ ) is analyzed for solvability of its Cauchy problem. The stipulations, including hyperbolicity with respect to initial values, are reformulated in Riemann invariants. The Born-Infeld system of equations, which belongs in the class of systems with identical principal parts, is then shown to have two sets of characteristics ( $r$ - $s$ -) both dependent on the initial conditions. These characteristics are families of parallel curves, any  $s$ -characteristic being an isocline for all  $r$ -characteristics and any  $r$ -characteristic being an isocline for all  $s$ -characteristics. Under non-zero initial conditions on the  $[x_1, x_2]$  segment, there correspondingly form two families of waves propagating in opposite directions with velocities  $+1$  and  $-1$  respectively. Under the additional constraint that  $\sum (\delta U_k / \delta)^2$  over  $k$  from 1 to  $n < 1$  at time  $t = 0$ , moreover, there is shown to exist a unique solution to the Cauchy existence defined on the whole in  $t$  and  $x$  within an arbitrary characteristic triangle where  $U_k$  in set  $C^2$  ( $k = [1, n]$ ). When the initial conditions are finite functions with a vector on that segment, then the initial perturbation decays into two families of plane solitary waves. Extension of the analysis to non-zero initial conditions on two nonintersecting segments yields a solution in the form of two families of plane solitary waves, these waves passing through an interaction space within a certain transit time. Three special sets of initial conditions corresponding to specific situations such as a relativistic string illustrate these conclusions. Two theorems are proved which validate the existence and uniqueness of a solution, the Cauchy problem under the given initial conditions on one segment and on two segments respectively. The author thanks B. M. Barbashov, V. V. Nesterenko, and V. V. Zharin for discussing relevant aspects of the subject. References 16.

### Photoneutrino Production on Nuclei in Strong Magnetic Field

917J0008B Moscow TEORETICHESKAYA I  
MATEMATICHESKAYA FIZIKA in Russian Vol 84  
No 2, Aug 90 pp 314-320

[Article by Yu. M. Loskutov and V. V. Skobelev, Moscow State University]

[Abstract] Fusion of photons on nuclei in the  $\gamma\gamma(Ze) \rightarrow \nu\nu(Ze)$  process in an ultrastrong magnetic field  $B \gg B_0 = m^2 / e$  ( $m$  - electron mass,  $e$  - electron charge) is analyzed in accordance with the Glashow-Weinberg-Salam model, calculations being greatly simplified by use of the two-dimensional field asymptote of quantum electrodynamics. The matrix element  $M\gamma\gamma(Ze) \rightarrow \nu\nu(Ze)$  is proportional to the ratio  $B/B_0$  so that in ultrastrong magnetic fields, photon fusion contributes more to production of neutrinos than does the one-photon process, even though photon fusion is described by diagrams of a higher order with respect to the coupling constant than the diagrams which

describe the  $\gamma(Ze) \rightarrow \nu\nu(Ze)$  process. This matrix element is calculated in the contact approximation, considering that the momenta of external electronic lines are smaller than those of internal electronic lines and that application of an external magnetic field  $B < m_W^2 / e$  ( $m_W$  - mass of gauge W-boson) does not invalidate this approximation inasmuch as the respective momentum integrals remain convergent. Physical characteristics of photon fusion are then calculated in the low-energy approximation, in which one invariant amplitude is  $R = -4\pi / 15m^6$ . The probability of photon fusion per unit time is obtained by integrating the matrix element  $\langle S | i$  with respect to momenta of neutrinos and averaging it over polarization states of photons. That probability is shown to depend on the angle between the resultant momentum of both photons and the direction of the magnetic field, namely to decrease as this angle decreases. Numerical estimates based on the realistic Glashow-Weinberg-Salam model ( $\sin^2\theta_W = 1/4$  where  $\theta_W$  - angle of W-boson momentum) indicate that, in an ultrastrong magnetic field, photon fusion produces more electron-neutrino than muon-neutrino pairs and the effect of neutral currents is to appreciably lower the probability of photon fusion. The probability of a crossover process is also calculated, and on that basis, the contribution of photon fusion to the luminosity of neutrinos produced concurrently by this and the one-photon process is then estimated. The results indicate that both processes are involved in the evolution of neutron stars and in the energy balance of collapsed objects. The authors thank A. Yu. Loskutov for processing the data on a computer. Figures 3; references 13.

#### Another Contribution of Order $\alpha^2(Z\alpha)E_F$ to Hyperfine Split in Muonium and in Hydrogen

917J0015A Moscow PISMA V ZHURNAL  
EKSPERIMENTALNOY I TEORETICHESKOY  
FIZIKI in Russian Vol 52 No 6, 25 Sep 90 pp 937-939

[Article by S. G. Karshenbaum, V. A. Shelyuto, and M. I. Eydes, Scientific Research Institute of Metrology imeni D. I. Mendeleev]

[Abstract] Corrections accounting for contributions to hyperfine split in muonium and in hydrogen are considered, once all purely radiative ones of the  $\alpha^2(Z\alpha)E_F$  order had already been calculated and shown to correspond to six gauge-invariant sets of diagrams with two external photons. Corrections corresponding to polarization operator inserts into the external photon lines have also been calculated and shown to correspond to three gauge-invariant sets of diagrams. The last correction corresponding to vacuum polarization inserts are now calculated on the basis of a compact relation for the sum of single-loop radiative corrections to the electron line with emission of two photons. They are  $\delta E_{Mu,H} = -0.310742... \alpha^2 Z \alpha E_F^{Mu,H} / \pi \cong -0.17$  kHz for Mu and -054 kHz for H. Figures 1; references 8.

#### Spontaneous Formation of Autosolitons in Stable Unbalanced Systems

917J0015B Moscow PISMA V ZHURNAL  
EKSPERIMENTALNOY I TEORETICHESKOY  
FIZIKI in Russian Vol 52 No 6, 25 Sep 90 pp 945-951

[Article by B. S. Kerner and S. L. Klenov]

[Abstract] The probability of spontaneous formation of autosolitons in unbalanced systems, originally stable under small perturbations of their parameters, is calculated on the basis of the Kerner-Osipov equation (USPEKHY FIZICHEKIKH NAUK Vol 157, 1989) describing such systems, considering that deviations of parameters in a uniform state satisfy the Ginzburg-Landau equation for the time derivative of their amplitude and with a correction added to account for small local inhomogeneities always existing in real physical systems. For a one-dimensional, an excited system is first considered the range of system excitation levels  $A$  near the critical level  $A_c$  above which the system becomes unstable, namely  $(A_c - A) / A_c \ll 1$ . Stationary distributions of the parameter deviation amplitude  $W$  near an inhomogeneity are found to exist only when the system excitation level  $A$  does not exceed a second critical one  $A_c^- < A_c$ . Random motion of a "particle" in a potential  $V(u) = u\delta - bu^3 / 3$  is described, this potential having two extrema at points  $u_m^{+-} = \pm(\delta/b)^{1/2}$  respectively which correspond to nonstationary (+) and stationary (-) distributions of deviation amplitude  $W$  at excitation levels  $A < A_c^-$ . Subsequently, the waveform of critical fluctuations of the finite parameter deviation amplitude  $W$  under a random force is determined; increases of this amplitude lead to spontaneous formation of an autosoliton. The probability per unit time of autosoliton formation will then, in the limit of a very weak noise, begin to increase infinitely as the range of  $u > u_m^+$  is reached. Figures 2; references 7.

#### Results of Measurements of Neutron Lifetime With Gravity Trap of Ultracold Neutrons

917J0017A Moscow PISMA V ZHURNAL  
EKSPERIMENTALNOY I TEORETICHESKOY  
FIZIKI in Russian Vol 52 No 7, 10 Oct 90 pp 984-989

[Article by V. Ye. Varlamov, A. V. Vasilyev, V. P. Gudkov, V. V. Nesvizhevskiy, A. P. Serebrov, S. O. Suzhbayev, R. R. Taldayev, and A. G. Kharitonov, Institute of Nuclear Physics imeni B. P. Konstantinov, USSR Academy of Sciences, V. P. Alfimenkov, V. I. Lushchikov, A. V. Strelkov, and V. N. Shvetsov, Joint Institute of Nuclear Research]

[Abstract] New measurements of the neutron lifetime were made by the method of confining ultracold neutrons in a gravity trap. The measurements were made at temperatures as low as 15 K with weakly absorbing substances such as beryllium and oxygen so as to minimize loss of ultracold neutrons by inelastic scattering during their storage and decay. The traps were made of aluminum, their inside surface coated with a 300 - 500

nm thick beryllium film and the latter either bare or covered with a 3 - 7  $\mu\text{m}$  thick layer of frozen 99.99 percent pure oxygen. With a spherical trap 75 cm in diameter used in the first part of the experiment, the probability of inelastic neutron scattering was equal to only 3 percent of the probability of neutron  $\beta$ -decay so that the neutron lifetime could be measured almost directly. With a cylindrical trap 72 cm in diameter and only 15 cm high used in the second part of the experiment the range of values of  $\gamma(E, R, E_{\text{lim}})$  ( $E$  - neutron energy,  $E_{\text{lim}}$  - limiting energy of trap wall,  $R$  - characteristic dimension of trap) in the equation for the neutron lifetime was extended without loss of precision, namely by also changing  $R$  in addition to varying  $E_{\text{lim}}$ . The results of these measurements fit the relation  $1/\tau_s = 1/\tau_n + \eta\gamma$  ( $\eta$  - neutron loss factor,  $\tau_s$  - storage time,  $\tau_n$  - neutron lifetime). They have yielded a neutron lifetime of 888.4  $\pm$  2.9 s, which corresponds to a  $G_A / G_V = \lambda = -(1.2677 \pm 0.0025)$  ratio of weak-interaction axial constant to vector constant, while the ratio  $\lambda_A$  based on measurement of the electron-spin asymmetry factor is  $-(1.2570 \pm 0.0028)$  so that the difference between the two values is within  $3.2\sigma$ . Figures 3; references 23.

### New Representation of Hubbard Model

917J0017B Moscow PISMA V ZHURNAL  
EKSPERIMENTALNOY I TEORETICHESKOY  
FIZIKI in Russian Vol 52 No 7, 10 Oct 90 pp 999-1002

[Article by G. G. Khaliullin, Kazan Institute of Engineering Physics imeni Ye. K. Zavoyskiy, Kazan Science Center, USSR Academy of Sciences]

[Abstract] Another representation of the t-J Hamiltonian which describes the Hubbard model at the  $U \gg t$  limit is proposed, namely one without additional equations coupling the operators which describe spin and charge degrees of freedom. This representation, particularly useful for systems with low electron concentration, involves the spinless fermion operator of hole or electron-hole pair generation and the local pseudospin representing the real spin in singly occupied nodes during motion of fermions. With the aid of this Hamiltonian, it becomes possible to calculate physical quantities by the standard method without complicated equations of coupling. The quasiparticle spectrum is accordingly calculated in the low-concentration limit ( $\delta < \delta^*$ ,  $\delta^* \approx 0.04$  when  $t/J = 3$ ), starting from the Néel state (zero absolute temperature) and with the Hamiltonian expressed through sublattice-symmetric magnons in the linear approximation. For concentrations  $\delta > \delta^*$  is then used the phenomenological concept of a rotation-invariant spin liquid phase with a short-range antiferromagnetic order and the corresponding static correlator when  $R \rightarrow \infty$ . Hyperfine interaction, which determines nuclear relaxation, is calculated next. The imaginary part of the expression for the one-point spin susceptibility involved in this interaction consists of a Fermi liquid term and a pseudospin term, the latter being the principal contributor to nuclear relaxation. Softening of magnons within the  $\delta > \delta^*$  range and their logarithmic infrared behavior

in the  $\delta > \delta^*$  range indicate a strong coupling between fermions and the boson field throughout the  $\delta \leq \delta^*$  range. This study was made within the scope of Project N 344 in the Government Program "High-Temperature Superconductivity" supported by Science Council. References 3.

### Charge Relaxation on Fractal Structures

917J0017C Moscow PISMA V ZHURNAL  
EKSPERIMENTALNOY I TEORETICHESKOY  
FIZIKI in Russian Vol 52 No 7, 10 Oct 90  
pp 1007-1009

[Article by V. Ye. Arkhincheyev, Buryat Science Center, Siberian Department, USSR Academy of Sciences]

[Abstract] Charge relaxation on regular fractal structures is analyzed: An equation in fractional time derivatives which describes the relaxation as being derived with the aid of renormalization group transformations from the fundamental system of equations  $\delta\rho / \tau + \text{div } j = 0$  ( $j = \sigma e$ ,  $\rho$  - excess charge density,  $j$  - electric current,  $e$  - electric field intensity,  $\sigma$  - electrical conductivity of medium) which describes charge relaxation in a conducting medium. Scale transformations of this system of equations are performed by changing to the  $\lambda$ -representation in time and converting the space derivatives into finite differences. As specific examples of fractal structures, Sierpinski gaskets and Koch curves are considered. The resulting equation  $\delta^S \rho / \delta t^S + \rho = 0$  indicates that charge relaxation over long time periods, in the low-frequency limit, follows a power law rather than the Maxwellian exponential law. This being consistent with the fact that fractal structures have no characteristic dimensions, charge relaxation therefore can occur on metal inclusions of all possible sizes. The equation also describes charge relaxation on percolation clusters at the conduction threshold. References 5.

### New Constraints on T-Invariance Breaking in $\beta$ -Decay

917J0018A Moscow PISMA V ZHURNAL  
EKSPERIMENTALNOY I TEORETICHESKOY  
FIZIKI in Russian Vol 52 No 9, 10 Nov 90  
pp 1065-1068

[Article by I. B. Khriplovich, Institute of Nuclear Physics, Siberian Department, USSR Academy of Sciences]

[Abstract] Stringent constraints on the imaginary parts of T-invariance breaking nucleon-lepton  $\beta$ -decay constants having already been established, namely  $\text{Im}[C_T + C_T'] < 0.5 \times 10^{-3}$  for the tensor constant,  $\text{Im}[C_s + C_s'] < 4 \times 10^{-3}$  for the scalar constant, and  $\text{Im}[C_p + C_p'] < 0.3$  for the pseudoscalar constant, constraints are now established on the imaginary parts of T-invariance breaking  $\beta$ -decay weak-magnetism ( $m$ ) and weak-dipole ( $e$ ) constants. For these constants in quark-lepton  $\beta$ -decay, the earlier constraint  $\text{Im}[\tilde{g}_{m,e}] < 10$  is refined to  $< 10^{-4}$  and

for these constants in nucleon-lepton  $\beta$ -decay the constraint is then also  $\text{Im}[g_{m,e}] < 10^{-4}$ , even with a conservatively estimated truncation parameter  $\Lambda$  of the order of 100 GeV. As to the weak nucleon current generated by  $T$  invariance breaking in hadron-hadron interaction, its possible contribution to the  $T$ -odd  $\text{Im}[g_{m,e}]$  constants should be even smaller than  $10^{-4}$ . Constraints on  $T$ -odd  $P$ -even nucleon-nucleon interaction have already been established, namely 10 G according to the one-loop diagram and  $10^{-4}$  according to the two-loop diagram. The author thanks L. de Braeckeleer for calling attention to this problem. Figures 3; references 6.

### Limits on Neutrino Oscillation Parameters for Reactor Antineutrinos

917J0025 Moscow ZHURNAL  
EKSPERIMENTALNOY I TEORETICHESKOY  
FIZIKI in Russian Vol 98 No 3(9), Sep 90 pp 764-768

[Article by G. S. Vidyakin, V. N. Vyrodov, I. I. Gurevich, Yu. V. Kozlov, V. P. Martemyanov, S. V. Sukhotin, V. G. Tarasenkov, and S. Kh. Khakimov, Institute of Atomic Energy imeni I. V. Kurchatov]

[Abstract] In an experiment concerning neutrino oscillations, a reverse  $\beta$ -decay on a proton was recorded:  $\bar{\nu}_e + p \rightarrow n + e^+$ , only neutrons produced by this reaction had been recorded. The integral detector of reactor antineutrinos was made of aluminum in the form of a 50 cm wide and 110 cm high right parallelepiped, filled with granules of polyethylene and a hexagonal bundle of 90 low-noise proportional  $^3\text{He}$  neutron-counter rods forming a center core along one of the two horizontal axes, wrapped with an at least 40 cm thick jacket of borated polyethylene as passive shield against ambient noise, and covered on top with PMMA (polymethyl methacrylate) scintillator plates as active shields against cosmic mesons. The experiment involved three reactors respectively—57.0 m, 57.6 m, and 231.4 m away from the detector. It lasted about 11,760 h and covered all 8 possible combinations of reactor states (on-on-on, on-on-off, on-off-on, on-off-off, off-on-on, off-on-off off-off-on, off-off-off). The data have been normalized to one series of readings and the latter formalized into a system of eight linear equations in four variables: Readings of neutron events in the three reactors and detector hum (neutrons produced in it plus those  $\alpha$  particles produced in the counters which reach amplitude window). This system of equations is thus an indeterminate one and, therefore, solved by the method of chi-square minimization. The results of this experiment, together with those of a previous experiment (first reactor 32.8 m away from the detector), yield upper bounds for the neutrino oscillation parameters  $\Delta^2 \leq 8.3 \times 10^{-3} \text{ eV}^2$  in the  $\sin^2(2\theta) = 1$  configuration and  $\lambda = G_A / G_V = 1.24 \pm 3.4$  percent (90 percent confidence level). The authors thank S. T. Belyayev for interest and helpful discussions, Ye. V. Turbin, A. Yu. Chechekin, A. I. Kireyev, I. V. Panov, and E. V. Lykhin for assistance in setting and performing the experiment, and the staff at the reactor facility for ensuring favorable work conditions. Figures 2; references 8.

### Masses of Quarks and Leptons in Model With Discrete Symmetry

917J0027A Moscow PISMA V ZHURNAL  
EKSPERIMENTALNOY I TEORETICHESKOY  
FIZIKI in Russian Vol 52 No 10, 25 Nov 90  
pp 1115-1118

[Article by N. I. Polyakov, Institute of Experimental and Theoretical Physics]

[Abstract] For a natural explanation of the observed mass hierarchy of quarks and leptons including a 77 GeV lower-bound for the  $t$ -quark mass, 12 physical quantities are reconstructed with the minimum number of trimmer parameters on the basis of the model with discrete  $Z_n$  symmetry with the requirement that all the Yukawa constants responsible for  $Z(2^p) \rightarrow Z(2^q)$  symmetry breaks are equal for all  $q$ 's. The model contains  $1 + n$  Higgs doublets ( $n = 2^p$ ,  $p = 14$ ), a group of their cyclic permutations yielding the  $Z_n$  symmetry and the latter, in turn, determining the form of the Yukawa relations. Fermion mass matrices are derived from this model by insertion of the appropriate column vectors describing the  $Z_n$  charges of quarks and leptons into the Yukawa relations for  $d$ -quarks,  $u$ -quarks, and leptons. The column vectors for quarks have been formulated so as to make  $q_3 - u_3 = 0$  and thus allowing for the possibility of a Yukawa relation between a  $t$ -quark and a  $Z_n$  singlet, Higgs doublet as well. Diagonalization of the fermion mass matrices yields the elements of the quark mixing matrix. These in turn yield the masses of all six quarks ( $u, d, c, s, t, b$ ) and of three leptons ( $e, \mu, \tau$ ), with the mass of a  $t$ -quark assumed to be  $m \approx 140$  GeV for reference. The author thanks K. A. Ter-Martirosyan for the many discussions. References 5.

### Phase Transitions and New Kinds of Ordering in Ising Model With Random-Field Defects

917J0027B Moscow PISMA V ZHURNAL  
EKSPERIMENTALNOY I TEORETICHESKOY  
FIZIKI Vol 52 No 10, 25 Nov 90 pp 1135-1137

[Article by Ye. B. Kolomeyskiy, Institute of Crystallography, USSR Academy of Sciences]

[Abstract] Considering that the lowest critical dimensionality of the Ising model with random-field defects has been recently proved to be  $d = 2$ , which corresponds to an initially uniform magnetized state which becomes unstable upon fragmentation into domains when the disorder is negligible, a phase transition will evidently occur as the disorder increases when the dimensionality is any  $d > 2$ . A theory of such a phase transition, similar to the scaling theory of Anderson localization, is constructed by analyzing the dependence of both the surface tension coefficient  $\sigma$  and the excess energy (called total stiffness)  $G$  of a domain wall on the linear scale  $L$ , especially when  $L \rightarrow \infty$ . This theory is then refined by introduction of the Gell-Mann-Low function  $d \log G / d \log L$  and extended to the  $1 < d \leq 2$  range, within which the theory predicts new phase transitions not of the Ising type. Figures 2; references 2.

### Use of Multilayer Structures as Targets for Generating Collimated X-Ray Quantum Beams

917J0004B Leningrad PISMA V ZHURNAL  
TEKHNICHESKOY FIZIKI in Russian Vol 16 No 15,  
12 Aug 90 pp 43-47

[Article by Yu. I. Dudchik, F. F. Komarov, M. A. Kumakhov, D. G. Dobotskiy, V. S. Solov'yev, and V. S. Tishkov]

[Abstract] Using multilayer structures as targets for generating narrow collimated beams of bremsstrahlung and characteristic x-ray beams is demonstrated, use of these structures for the transportation or the focusing of hard x-rays or  $\gamma$ -rays and for generating intermediate x-rays had previously been proposed. The feasibility has been demonstrated in an experiment with a Ta-Al-Ta-Al-Ta-Al-Ta stack on a Si substrate and normally incident 0.1 - 1 MeV electron beams. The emission coefficient for radiation from a Ta layer ("heavier" material with smaller refractive index) into an Al-layer ("lighter" material with larger refractive index) and the reflection coefficient for photons at the Ta-Al boundaries on the Al side, both depend on the glancing angle, but adiabatically, with a crossover when the glancing angle is equal to the critical (total external reflection) angle. Bremsstrahlung, or x-rays, pass from a Ta-layer to an Al-layer, through which they then propagate, mostly at glancing angles larger than the critical. They leave an Al-layer, after multiple reflections, mostly at glancing angles smaller than the critical. The layers of "heavier" material thus act as moderators and walls of a bremsstrahlung or x-ray waveguide with the "lighter" material as filler. These walls must obviously be sufficiently thick for total external reflection to occur. Inasmuch as the interlayer interfaces are not perfect, anomalous Ioned scattering by rough surfaces will boost the intensity of radiation propagating through such a waveguide. Figures 3; references 6.

### Fractal Characteristics of Percolation Conduction in Polycrystalline PbS Layers

917J0016C Moscow PISMA V ZHURNAL  
EKSPERIMENTALNOY I TEORETICHESKOY  
FIZIKI in Russian Vol 52 No 5, 10 Sep 90 pp 917-920

[Article by O. A. Gudayev, V. K. Malinovskiy, and E. E. Paul, Institute of Automation and Electrometry, Siberian Department, USSR Academy of Sciences]

[Abstract] Charge transfer in materials with strongly nonuniform properties is analyzed using the concepts of percolation clusters and their fractal structure. The material, polycrystalline PbS, is considered in which the mean free path is of the order of the interatomic distance and the charge carrier mobility is of the order of  $1 \text{ cm}^2 / (\text{V}\cdot\text{s})$ . The analysis is based on treating the charge transfer as a diffusion process or Brownian movement (M.H. Cohen, J. NONCRYSTALLINE SOLIDS Vol 36, 1970), without localization, but not a free motion. The diffusion coefficient  $D_g$  on a fractal is defined as a

function of the distance  $r$ , namely  $D_g(r)$  proportional to  $r^{-2(D/d - 1)}$  ( $D$  - Hausdorff fractal dimensionality,  $d$  - spectral dimensionality), and the mobility is estimated according to the Einstein relation  $\mu = eD_g/kT$ . Transfer of excess charge carriers in a semiconductor by a percolation cluster which has a fractal structure is then considered, their "random travel" time being equal to their mean life  $\tau$ . The photoconductivity of such a material is then  $\sigma_p$  proportional to  $\tau^p$ , where  $p = 2 - d/D$  and  $d = 4/3$  universally for all percolation systems. This result was verified experimentally on films of the photosensitive PbS semiconductor material. The mean life  $\tau$  of excess carriers was determined on the basis of photocurrent measurements after excitation by a light pulse, namely by tracking the photocurrent decay as a function of time. The photoconductivity of this material was then calculated according to the relation  $\sigma_p = e\alpha I \mu(T, \tau) \tau$  ( $e$  - carrier charge,  $\alpha$  - absorption coefficient,  $I$  - light intensity), the carrier mobility  $\mu(T, \tau)$  depending on both the mean carrier life and the temperature  $T$ . Measurements were made at temperatures covering the 77 - 293 K range. The films were excited with light quanta  $h\nu$  larger than the energy gap  $E_g$  in PbS and thus, a wavelength shorter than 950 nm so as to eliminate the temperature dependence of the absorption coefficient due to shifting of the edge of the fundamental absorption band. The temperature dependence of the carrier mobility was eliminated by normalizing the photoconductivity at any given temperature to the dark conductivity. The data indicate that, while the mean life of excess carriers becomes shorter and the dark conductivity increases with rising temperature, the photoconductivity peaks at about 170 K. As the intensity of incident light is increased,  $d/D$  decreases so that  $p$  increases and when it reaches 1.6 the nonlinear dependence of the photoconductivity on the mean carrier life then begins to correspond to a fractal structure of percolation clusters. Figures 2; references 5.

### Theory and Numerical Simulation of Optical Properties of Fractals

917J0025B Moscow ZHURNAL  
EKSPERIMENTALNOY I TEORETICHESKOY  
FIZIKI in Russian Vol 98 No 3(9), Sep 90 pp 819-837

[Article by V. A. Markel, L. S. Muratov, and M. I. Shtokman, Institute of Automation and Electrometry, Siberian Department, USSR Academy of Sciences]

[Abstract] A theory of optical properties of fractals is constructed, a fractal being regarded as an array of  $N$  polarizable monomers with dipole-dipole interaction at optical frequencies and its fluctuation characteristics fully accounted for. An exact relation is derived from the exact solution to the known system of equations for dipole moments induced on monomers, an analog of the optical theorem, which yields the mean-cluster local electric field acting on a monomer. This electric field determines both amplified Raman scattering by a cluster and photoinduced modification of a cluster. An exact rule of sums is then obtained upon consideration of rotational symmetry. The polarizability of a fractal in

the collective region is calculated next, considering that a fractal is a self-similar absorption object. Its imaginary part, representing optical absorption, is a power function of the variable  $X = h\Omega|d_{12}|^2$  ( $d_{12}$  - dipole moment,  $\Omega = \omega - \omega^0$  - frequency deviation from monomer resonance,  $h$  - Planck constant). Its real part is shown not to be a power function of  $X$  but to cover the collective region where  $|X| \ll 1$  and both tails of the absorption region  $|X| \gg 1$ . These tails of the fractal spectrum are described in accordance with the dilution (random decimation) model, in the binary approximation. The optical properties of three kinds of fractals were studied by numerical simulation, all fractals had been obtained by the Monte Carlo method with the aid of programmable random numbers generator. Random walks ( $D = 2$ ) were constructed on a cubic grid with monomers stopping in nodes and then diluted by a factor of 1000 into clusters of an average of 30 monomers. Random walks without self-crossings were constructed by the trial and error method using a step of constant length and random orientation, with monomers placed in nodes and treated as not interpenetrable identical spheres (diameter equal to step), then diluted by a factor of 20 into clusters of an average of 25 monomers. Fractals of the third kind, Witten-Sander clusters, were constructed by simulation of diffusion-controlled aggregation on a cubic grid and then diluted by a factor of 20 into clusters of an average of 25 monomers. Numerical simulation of these fractals has yielded spectral variable  $z = -X - i\delta$  having been selected the reverse polarizability of a solitary monomer and  $X = 0$  corresponding to its resonance frequency. Theoretical analysis of the results has yielded for amplification of the local electric field acting on a monomer a gain  $G$  asymptotically equal to  $|X|^{d(0)+1} / \delta$  in the collective region and to  $|X|^{1-D/3} / \delta$  in the tail regions of diluted fractals in the binary approximation. The results indicate that earlier predicted large fluctuations of local fields and consequently giant amplification of Raman or parametric scattering are not artifacts of the binary approximation but a common property of all nontrivial fractals whose component monomers act as high-Q optical resonators. The authors thank A. V. Butenko, V. I. Safonov, and V. M. Malayev for helpful discussions. Figures 7; references 19.

#### Generation of Nonlinear Surface Waves by Electromagnetic Beams

917J0035A Moscow ZHURNAL  
EKSPERIMENTALNOY I TEORETICHESKOY  
FIZIKI in Russian Vol 98 No 4(10), Oct 90  
pp 1191-1203

[Article by Ya. L. Bogomolov, A. V. Kochetov, A. G. Litvak, and V. A. Mironov, Institute of Applied Physics, USSR Academy of Sciences]

[Abstract] Generation of nonlinear surface waves by electromagnetic beams at the boundary between a linear medium and a nonlinear one is analyzed; the optically less dense medium being nonlinear when its dielectric

permittivity increases in the presence of an electric field and a surface wave then representing the solution to the system of Maxwell equations at that boundary. Propagation of a Gaussian electromagnetic beam along the boundary between such media is considered and the conditions are established under which its transformation into nonlinear surface waves can occur. The problem is tackled first for steady-state case on the basis of an analogy to a noninertially nonlinear medium. A stability analysis of the solution to the corresponding system of two wave equations indicates that the nonlinear surface wave will be stable when  $\alpha_n < 2$  and unstable when  $\alpha_n > 2$ . The parameter  $\alpha_n$ , which combines the propagation constant and the real parts of dielectric permittivity in each medium, coincides with the Kolokov-Vakhitov criterion for self-focusing in a boundless medium. An analysis of steady-state wave generation based on the first moment of the field distribution yields the optimum parameters of a Gaussian beam, its trajectory being determined by the dependence of the potential profile in the nonlinear medium on the beam amplitude. Relevant to the generation of nonlinear surface waves is a beam most of whose power has been initially concentrated in the linear medium. The system of two wave equations has been solved numerically after conversion into difference equations according to the Crank-Nicholson scheme, the results indicating that a nearly 100 percent efficient beam-to-wave transformation is attainable with optimum beam parameters. Analysis of dynamic wave generation by a Gaussian beam is based on the assumption of a beam stabilization time (transient period), much shorter than the nonlinear medium characteristic relaxation time, so that the field can be described by those steady-state equations with  $\Delta\epsilon E$  replacing  $|E|^2 E$  ( $\epsilon$  - dielectric permittivity) and the equation  $\Delta\epsilon + \delta\Delta\epsilon/dt = |E|^2$ . This equation and the equation for the second moment of the field distribution, effective beam width squared, has been solved numerically using an implicit scheme of discrete Fourier transformation. The results indicate that a Gaussian beam can generate an unstable nonlinear surface wave which will become a stable one, with attendant formation of a steady beam which will move into the linear medium. Figures 6; references 21.

#### "Direct Viewing" of Atomic Structure of Crystal Under High-Resolution Electron Microscope

917J0035B Moscow ZHURNAL  
EKSPERIMENTALNOY I TEORETICHESKOY  
FIZIKI in Russian Vol 98 No 4(10), Oct 90  
pp 1402-1411

[Article by V. L. Indenbom and S. B. Tochilin, Institute of Crystallography imeni A. V. Shubnikov, USSR Academy of Sciences]

[Abstract] Direct viewing of the atomic structure of a crystal under a high-resolution electron microscope with normal transillumination is discussed, considering that normal transillumination gives rise to all Bloch waves of the ns-series ( $n = 1, \dots, \infty$ ) simultaneously so that only

images of atomic chains indicated by the central peaks of ns-waves, but also "spurious" maxima, are seen. An example are the distinct annular halos appearing, instead of brightness maxima, on the microphotograph of a crystalline gold foil (H. Hashimoto, H. Endoh, T. Tanji, et al.; J. PHYSICS SOCIETY OF JAPAN Vol 42, 1977), their nature having so far been only speculated about. The authors have proposed and are now proving that these halos are produced by interference effects in the wave field inside such a foil, as fast electrons passing through it are channeled around the periphery of potential wells. Another example are the lateral brightness spikes appearing between atoms on the microphotograph of a  $\text{Si}_3\text{N}_4$  crystal (Center of Materials Science at Mining School in Paris) under Dutch microscope with 0.2 nm resolution, declared by those researchers to be a "glassy phase within the  $\text{Si}_3\text{N}_4$  structure" but here shown to be regular diffractive brightness spikes at the boundaries of unit cells, two-dimensional in projection, or of Voronov zones in the actual crystal. The theoretical part of the proof is based on the mathematical model of coupled ns-Bloch waves, graphical representation of ns-Bloch functions demonstrating how images of halos appear while images of atomic chains vanish. The experimental part of the proof is a photograph showing brightness spikes where there are no atoms and showing most distinctly the corners of unit cells farthest from the atomic chains on which bound Bloch chains have centered. Direct viewing of the atomic structure is evidently not possible at this state of the art when the crystal contains chains of both heavy and light atoms. Figures 6; references 12.

#### Theory of Acceleration of Charged Particles by Ensemble of Shock Waves in Turbulent Medium

917J0035C Moscow ZHURNAL  
EKSPERIMENTALNOY I TEORETICHESKOY  
FIZIKI in Russian Vol 98 No 4(10), Oct 90  
pp 1255-1268

[Article by A. M. Bykov and I. N. Toptygin, Leningrad Polytechnic Institute imeni M. I. Kalinin]

[Abstract] A theory is constructed to describe the kinetics of charged particles interacting with and accelerated by an ensemble of shock waves in a turbulent interstellar medium, assuming a uniform and steady supersonic turbulence. The ensemble is considered to be a random one, statistically uniform and isotropic, with a given mean distance between wavefronts propagating at velocities equal to or higher than  $N_{Ma}$ , but no more than 2. A cloud of charged particles with a wide power-law energy spectrum forms near each wavefront as they are accelerated by it. The distribution function of these particles averaged over the ensemble of wavefronts takes into account the strong local inhomogeneities in that cloud, assuming that their length scale  $l$  is much smaller than the mean distance between wavefronts  $L$ . The distribution function is averaged first over length scales  $\Delta$  within the intermediate range, much larger than  $l$  and much smaller than  $L$ , then over large-scale movements of the turbulent

medium. Inasmuch as diffusion associated with small-scale turbulence plays a minor role here, this diffusion is assumed to be constant in time and isotropic in space. The tensor of turbulent diffusion coefficients and three coefficients which determine the rate of acceleration are calculated on this basis in the form of integrals. In the case of slow acceleration, the entire velocity field is included in the averaging of the distribution function, after an auxiliary problem of perturbation theory has been solved. In the case of fast acceleration, corresponding to large changes of particle energy within the turbulence velocity correlation time, acceleration not only at the wavefronts but also between them is described by an integral operator. Stationary energy spectra of particles accelerated by an ensemble of shock waves and also by large-scale turbulent movements are calculated, after a source of monoenergetic particles has been included in the equation for the complete distribution function and with leakage of particles from the acceleration zone taken into account. These spectra are most conveniently calculated by performing first a Fourier and then an inverse Fourier transformation. References 14.

#### Control of Fermi Level and Phase Transitions in $\text{YBa}_2\text{Cu}_3\text{O}_{7-d}$ Material

917J0035D Moscow ZHURNAL  
EKSPERIMENTALNOY I TEORETICHESKOY  
FIZIKI in Russian Vol 98 No 4(10), Oct 90  
pp 1375-1381

[Article by Yu. M. Gerbshteyn, N. Ye. Timoshchenko, and F. A. Chudnovskiy, Institute of Engineering Physics imeni A. F. Ioffe, USSR Academy of Sciences]

[Abstract] An experimental study of  $\text{YBa}_2\text{Cu}_3\text{O}_{7-d}$  material was made concerning control of the Fermi level by regulation of the equilibrium oxygen pressure on the surface; the pressure stabilizing quite quickly and the chemical potential of electrons in the material and that of electrons in the gaseous oxygen then becoming equal during heat treatment at temperatures within the 450 - 500°C range. Subsequent measurements revealed how the mass  $m$  of a specimen, the density of electron states  $\delta N/E_F$  in it, the lattice constants  $a, b, c$ , the superconducting transition temperature  $T_c$ , the electrical resistance  $R_{300K(\text{room})}$ , and the resistance activation energy characterizing transition to the dielectric state depend on the Fermi level. Measurements were made on specimens with  $d = 0.7$  and with  $d = 0$ . According to theory, the number of electronic states within a  $\Delta E_F$  interval is  $\Delta N = 2\Delta x$  when the oxygen is bivalent and  $\Delta N = n\Delta x$  when the oxygen is less than bivalent ( $\Delta x$  - number of oxygen atoms,  $n$  - effective valence of oxygen). The amount of oxygen was determined in two ways: 1) by weighing before and after heat treatment, and 2) with a superionic oxygen pump. The number of electronic states was then calculated so that the function  $D(E_F) = \Delta N/\Delta E_F v$  ( $v$  - volume of specimen) could be evaluated over a wide range of  $E_F$ . The results indicate that, as the Fermi level is raised, there occurs a sequence of transitions from the conducting state through Anderson localization to the

dielectric state. During the equilibrium stabilization process at temperatures above 500°C, there occurs a change of the oxygen content not only in chains but also in planes. On the basis of these results, the regions of existence have been established for the three orthorhombic-1, orthorhombic-2, and tetragonal phases on the  $E_F$  mass diagram. There evidently exists a relation between

the change of mass and the structure of the electronic spectrum. The anomalously high deformation potential in the superconducting orthorhombic-1 phase and in the tetragonal phase is shown to be attributable to the proximity of the respective structural phase transitions. The authors thank M. S. Bresler and B. P. Zakharchenko for interest and helpful discussions. Figures 6; references 6.

UDC 533.9

### Low-Frequency Potential Instabilities of Mutually Penetrating Electron Beams in Magnetic Gaps of Magneto-electrostatic Traps

917J0002A Kiev UKRAINSKIY FIZICHESKIY ZHURNAL in Russian Vol 35 No 8, Aug 90 pp 1187-1193

[Article by I. Ya. Gordiyenko, V. D. Yegorenkov, and K. N. Stepanov, Kharkov University imeni A. M. Gorkiy]

[Abstract] The presence of an uncompensated space charge of electron beams in the magnetic gaps of magneto-electrostatic traps results in the development of diocotron instability. The presence of opposing motion of electron beams can lead to excitation of low-frequency dual-beam instability. This work summarizes the results of previous studies in this area and constructs a theory of low-frequency potential electron beam instability in these magnetic gaps. Conditions are determined under which unstable diocotron oscillations and dual-beam low-frequency instability can occur. Expressions are derived for the frequencies and increments of low-frequency dual-beam instability with arbitrary placement of the electron layer relative to the conducting walls. Slight drift of electrons significantly decreases both the frequency and the increment of this instability, expanding the area of stability. Asymmetrical placement of the electron layer relative to the metal walls stabilizes both diocotron and low-frequency dual-beam instabilities. Figures 3; references 14: Russian.

UDC 537.312.62

### Substantiation of Quasi-One-Dimensional Bisoliton Model of Superconductivity of Ceramic Oxides

917J0002B Kiev UKRAINSKIY FIZICHESKIY ZHURNAL in Russian Vol 35 No 8, Aug 90 pp 1229-1235

[Article by A. S. Davydov, Institute of Theoretical Physics, Ukrainian Academy of Sciences, Kiev]

[Abstract] Recent studies by the author and his colleagues have developed a theory of high-temperature

superconductivity of oxides based on a quasi-one-dimensional model. The question arises of the applicability of this model to oxides not having segregated one-dimensional chains in the ab planes. This article demonstrates that the superconductivity of such crystals can also be described by the quasi-one-dimensional bisoliton model, according to which the charge carriers are bisolitons—quasiparticles (electrons or holes) paired in the singlet spin state. The bisolitons are distributed at equal distances from each other along a system of parallel lines with identical phases across these lines. This distribution of bisolitons in the crystal forms a quasi-one-dimensional superconducting condensate, which moves at constant velocity in the crystal. Figures 2; references 8; 1 Russian, 7 Western.

### Magnetic Traps With Conductors "Floating" in Plasma

917J0004C Leningrad PISMA V ZHURNAL TEKHNIЧЕСКОY FIZIKI in Russian Vol 16 No 15, 12 Aug 90 pp 86-89

[Article by A. I. Morozov, Institute of Atomic Energy imeni I. V. Kurchatov, Moscow]

[Abstract] Two versions of magnetic traps with conductors "floating" in the plasma are described, one with levitating conductors as well as conductors "standing" on the ground and one with conductors immersed in the plasma but with leads brought out of the plasma confinement and "standing" on the ground. Considering that a "baseball" coil can be designed to produce a magnetic field which will satisfy any given set of noncontradictory requirements ensuring both stability and equilibrium of the plasma, three reservations, nevertheless, have been raised as to the feasibility of using such coils in industrial thermonuclear reactors. These reservations are: 1) complexity of the magnetic suspension, 2) difficulties of extracting the "thermonuclear" energy, and 3) difficulties of sustaining superconductivity in the current-carrying conductors. It is demonstrated by the author that these reservations are unfounded. According to data on existing industrial D-T tokamaks with the first wall under heat loads of 1 - 2 MW/m<sup>2</sup> range, surface temperatures do not exceed the 2050 - 2440 K range when  $\epsilon = 1$ . A transverse magnetic field of about 100 Oe is shown to be sufficient for maintaining a current density of about 10 kA/cm<sup>2</sup> in a ceramic metal-oxide high-T<sub>c</sub> superconductor, with a density about 10 g/cm<sup>3</sup>, carrying a current of 3 MA and surrounded by a neutron shield 1 m in diameter made of a carbon-pyroceramic material with a density about 3 g/cm<sup>3</sup>. Figures 2; references 9.

### Production and Atomic Structure of Single-Domain Tm-B-Cu-O Superconductor

917J0006C Moscow PISMA V ZHURNAL  
EKSPERIMENTALNOY I TEORETICHESKOY  
FIZIKI in Russian Vol 52 No 4, 25 Aug 90 pp 854-858

[Article by V. I. Voronkova, V. K. Yanovskiy, V. N. Molchanov, N. I. Sorokina, and V. I. Simonov, Institute of Crystallography, USSR Academy of Sciences]

[Abstract] A study of  $\text{TmBa}_2\text{Cu}_{(3-x)\text{O}_{7-y}}$  superconductors was made, single-domain crystals having been grown from a nonstoichiometric crystal of the quasi-ternary  $\text{Tm}_2\text{O}_3$  -  $\text{BaO}$  -  $\text{CuO}(\text{Cu}_2\text{O})$  solid solution. The best crystals, without twinning during ferroelastic transition from the tetragonal high-temperature phase to the orthorhombic low-temperature phase, were obtained from a melt of 3 mol.%  $\text{Tm}_2\text{O}_3$  + 30 mol.%  $\text{BaO}$  + 67 mol.%  $\text{CuO}$  in corundum crystallizer with 5 - 10 ml capacity. Their domain structure was examined under an optical polarization microscope and by x-ray diffraction methods. A major factor influencing their superconductivity and lattice perfection was found to be the rate of cooling of crystals extracted from the melt. Cooling from 825 K to 525 K at 2 - 4 K/h without supplementary annealing in an oxygen atmosphere has yielded crystals with a critical temperature of 92 - 90 K within a 1 K wide superconducting transition range and with up to 1 mm large single domains free of twins. The atomic structure of a special specimen, a 14  $\mu\text{m}$  thick and 136 x 142  $\mu\text{m}^2$  large rectangular slice of a  $\text{TmBa}_2\text{Cu}_{2.972}\text{O}_{6.69}$  single crystal, was examined in a REM-4 diffractometer with a  $\text{Mo-K}_\alpha$  radiation source and a graphite monochromator by  $\omega$ -scanning at rates of 0.5 - 8.0°C/min. The much narrower temperature range of superconducting transition than that for Y-Ba-Cu-O compounds may be attributed to the fact that, as Y is replaced by Tm, the Cu-O layers remain the most stable ones in terms of interatomic distances and in terms of chemical bonds. While the Tm-O distances are smaller than the Y-O distances and the Ba-Ba distances increase, Cu(1)-O and Cu(2)-O distances change minimally. An exception is the Cu(2)-O(1) distance, which characterizes the weakest chemical bond and remains very labile. Figures 2; tables 1; references 7.

### Flux Creep and Depth of Pinning Centers in Organic Superconductor $k\text{-(BEDT-TTF)}_2\text{Cu}(\text{NCS})_2$

917J0016B Moscow PISMA V ZHURNAL  
EKSPERIMENTALNOY I TEORETICHESKOY  
FIZIKI in Russian Vol 52 No 5, 10 Sep 90 pp 914-917

[Article by V. D. Kuznetsov, Moscow Institute of Chemical Engineering imeni D. I. Mendeleev, V. V. Metlushko, Moscow State University imeni M. V. Lomonosov, L. A. Yepanechnikov and Ye. F. Makarov, Institute of Chemical Physics imeni N. N. Semenov, USSR Academy of Sciences, E. B. Yagubovskiy and N.

D. Kushch, Department of Institute of Chemical Physics imeni N. N. Semenov, USSR Academy of Sciences]

[Abstract] An experimental study of the organic superconductor  $k\text{-(ET)}_2\text{Cu}(\text{NCS})_2$  in the form of single crystals was made concerning the relaxation characteristic of its magnetic moment. Single crystals of this material were produced by electrochemical oxidation of BEDT-TTF in  $2 \times 10^{-3} \text{ mol/dm}^3$  strong 1,2-trichloroethane, on a platinum electrode with a constant current of 1.15  $\mu\text{A}$  at a constant temperature of 20°C. As electrolyte served the  $\text{Cu}(\text{SNC})\cdot\text{K}(\text{SNC})$  complex, freshly prepared by synthesis involving dissolution of  $\text{Cu}(\text{SNC})$  to a  $5 \times 10^{-3} \text{ mol/dm}^3$  in the 1:1:1 ratio. Measurements were made in a SQUID magnetometer. The intensity of the lower critical magnetic field  $H_{c1}$ , corresponding to departure of the magnetic moment  $P_m$  from linear dependence on the magnetic field intensity  $B$ , was found to be about 2.7 mT strong and the fraction of superconducting phase in a magnetic field of 3.7 mT at 4.2 K temperature was found to be about 15 percent. The magnetic moment  $P_m(t)$  as a function of time was measured after a crystal had been cooled to 4.2 K without a magnetic field (zero-field cooling) and a magnetic field then applied, its intensity being varied over the 2.17 - 20.54 mT range. The relaxation characteristic of the magnetic moment has been determined from the data, the relaxation rate  $R = dP_m/d(\log t)$  found to be constant at any constant magnetic field intensity within this range and to be maximum in a magnetic field of 3 mT intensity. Conversion to the referred rate of logarithmic relaxation  $S(B) = R\Delta P_m = kT / U_0 (\Delta P_m - \text{width of hysteresis loop proportional to the critical current})$  has yielded an average pinning energy  $U_0$  of about 7.2 meV in a magnetic field of about 6 mT intensity and decreasing with increasing magnetic field intensity  $B$ . The authors thank I. F. Shechegolev for helpful discussions. Figures 3; references 15.

### Critical Temperature for Ferromagnetic-Superconductor Superlattice

917J0018B Moscow PISMA V ZHURNAL  
EKSPERIMENTALNOY I TEORETICHESKOY  
FIZIKI in Russian Vol 52 No 9, 10 Nov 90  
pp 1089-1091

[A. I. Buzdin and M. Yu. Kupriyanov, Moscow State University imeni M. V. Lomonosov]

[Abstract] The critical temperature  $T_c^*$  for artificial superlattices of alternating ferromagnetic and superconductor layers, known to be nonmonotonically dependent on both the thickness of the ferromagnetic layers and the exchange field intensity in them, is for the first time determined analytically. Calculations are based on Uzdeli's (?) equations, assuming that both materials are "dirty" and that the ferromagnetic material is a normal metal with the critical temperature  $T_{cF} = 0$  K and with an exchange field intensity within the 100 - 1000 K range

far above the critical temperature  $T_{cS}$  for the superconductor material in bulk form. The system of three equations for such a superlattice in the vicinity of the critical temperature  $T_c^*$  involves the coherence lengths in the two materials, each proportional to the square root of the corresponding diffusion coefficient and inversely proportional to the square root of the critical temperature  $T_{cS}$ . It is supplemented with appropriate boundary conditions for the  $F_{s,n}^{+/-}(\omega)$  functions of the Matsubara frequency frequencies  $\omega = \pi T(2n + 1)$  at the superconductor-ferromagnetic interface. Only the two most important 0-phase and  $\pi$ -phase need to be considered, inasmuch as the intermediate range between them is very narrow. The problem can be further reduced to equations for only the two  $F_{s0,sn}^+$  functions. The critical temperature for the superlattice will then be either  $T_{c0}^*$  or  $T_{c\pi}^*$ , whichever is higher. The range of thicknesses of the ferromagnetic (normal metal) layers within which the 0-phase exists is then established in the approximations of a very small and very large parameter  $\gamma = \sigma_{NS}^{\xi_S^*} / \sigma_{SN}^{\xi_N^*}$  ( $\sigma_{S,N}$  - electrical conductivity of S and N materials,  $\xi_{N,S}^*$  - coherence length in N and S materials). The results indicate that a ground state with an order parameter whose phase varies from layer to layer can exist in an S-F superlattice. Formation of the 0-phase is favored when the thickness of the ferromagnetic layers is smaller than or, at most, equal to the coherence length in them and transition to the  $\pi$ -phase occurring as their thickness is made larger or the exchange field intensity in them decreases, their thickness at which this transition becomes smaller as the magnitude of  $\gamma$  increases. References 6.

### Mechanism of Frozen Photoconductivity in $YBa_2Cu_3O_{7-d}$ Superconductor

917J0022B Moscow PISMA V ZHURNAL  
EKSPERIMENTALNOY I TEORETICHESKOY  
FIZIKI in Russian Vol 52 No 8, 25 Oct 90  
pp 1049-1052

[Article by I. P. Krylov, Institute of Problems in Physics, USSR Academy of Sciences]

[Abstract] The recently discovered frozen photoconductivity in the  $YBa_2Cu_3O_{7-d}$  superconductor is attributed to oxygen deficiency and appearance of oxygen vacancies in the Cu1-O1 "chains". In an experiment with an Ar-laser, the electrical conductivity of a  $YBa_2Cu_3O_{7-d}$  crystal with  $d \approx 0.5$  increased by about 30 percent upon exposure to green light. With the crystal held at 100°C temperature, it retained this increment of electrical conductivity for an indefinitely long time after removal of the light source. This increment of electrical conductivity decreased to 50 percent within 20 h when the crystal was held at 295°C temperature and to 25 percent within 4 h when the crystal was held at 320°C temperature. The mechanism of frozen photoconductivity must be associated with deformation of the crystal lattice in the vicinity of a defect, which occurs as the electronic state of the defect changes. It is interpreted analytically on the basis of the electron Hamiltonian  $H = H_0 + \Sigma$

$(\delta H / \delta q_i) q_i$  over all  $i + \Sigma (\delta^2 / \delta q_i^2) q_i^2$  over all  $i$  ( $q_i$  - normal coordinates,  $i = 1, 2, 3, 4, 5$ ) and on the energy of an electron in the bound state plus the energy of elastic lattice deformation in the first-order perturbation theory, considering that the O1 position has point symmetry which belongs in the orthorhombic  $D_{2h}$ -group. Assuming that the displacements of atoms from their equilibrium positions  $u_j$  ( $j = 1, 2, 3, 4$ ) during transition from  $v = 0$  to  $v = 1$  ( $v$  - occupancy number of  $\epsilon_0$  level) are of the same order of magnitude as their displacements upon transition from a tetragonal  $YBa_2Cu_3O_6$  cell to an orthorhombic  $YBa_2Cu_3O_7$  cell, the radii of O, Cu, Ba, Y atoms being known, rough calculations in the adiabatic approximation are based on the model of solid spheres with the O1 oxygen atom freely occupying the interstice between four Ba atoms. A vacancy then creates an energy barrier surmountable by lattice vibrations. The temperature dependence of photoconductivity relaxation time has been described as an approximately exponential one (D.V. Lang), but owing the dependence of atom displacement on the Fermi level it is not exponential. If the vibron interaction were weak, moreover, the relaxation time could not possibly exceed 1 s even under most favorable assumptions. Figures 3; references 8.

### Low-Temperature Phase Transitions of First and Second Kinds in $YBa_2Cu_3O_{6+x}$ Due to Oxygen Redistribution Over Lattice Chains

917J0025C Moscow ZHURNAL  
EKSPERIMENTALNOY I TEORETICHESKOY  
FIZIKI in Russian Vol 98 No 3(9), Sep 90 pp 978-988

[Article by L. G. Mamsurova, K. S. Pigalskiy, V. P. Sakun, A. I. Shushin, and L. G. Shcherbakova, Institute of Chemical Physics imeni N. N. Semenov, USSR Academy of Sciences]

[Abstract] The high- $T_c$  superconductor materials  $YBa_2Cu_3O_{6+x}$  with  $x > 0.5$  are searched for possible stable ordered structures forming at low temperatures in the distribution of oxygen ions over lattice chains in the basis plane. The search relies on a theoretical model and on available experimental data, the latter revealing two phase transitions in this material at  $T \approx 1000$  K and  $T \approx 240$  K temperatures respectively. Only the region of the T-x constitution diagram for this  $YBa_2Cu_3O_{6+x}$  system needs to be considered which corresponds to the orthorhombic crystal structure, where the O5 positions are almost all empty and  $O^{2-}$  ions occupy O4 positions. Among those located in the same chain, only those in O4-Cu1-O4 pairs are assumed to attract each other and only those in different, neighboring, chains are assumed to repel each other pairwise, neither kind of interaction depending on the oxygen concentration. The problem then reduces to a scan of possible  $O^{2-}$  ion distributions over those plane chains and of three-dimensional structures which a sequence of such chains can form. The problem is solved with exact accounting for intracatenary thermodynamics and with treatment of the relatively weak intercatenary interaction in the mean-field approximation. Calculation of the incomplete free

energy  $F$  leads to the system of equations  $\delta F / \delta x_m = \mu$  ( $m = 1, 2, \dots, M$ ,  $\mu$  - chemical potential of  $m$ -th O4 chain relative to another one of the  $M$  chains in thermodynamically stable configuration). A stability analysis of the solution to this system of equations yields four stable periodic structures:  $O_I, O_{II}, O_{III}, O_{OIII}$ . The last two have triple-length periods with three elements in each repetitive group corresponding to oxygen concentrations  $x_1, x_2, x_3$ , the pattern being  $x_1 < x_2 = x_3$  and  $x_1 > x_2 > x_3$  respectively. Experimental data include the temperature dependence of Young's modulus  $E$ , acoustic loss due to internal friction  $Q^{-1}$ , measurements having been made on coarse-grain and ultrafine-grain specimens with  $x =$

0.9, 0.68, 0.55, 0.24. In some specimens with a high oxygen content the acoustic loss peaked at 240°C and a temperature hysteresis of Young's modulus was recorded in the vicinity of 200°C, this hysteresis indicated a phase transition of the first kind. Noteworthy is an evident correlation between the magnitude of maximum acoustic loss in specimens with  $x \rightarrow 1$  and the loop width (in °C) of their modulus hysteresis, the loop being widest below 240 K when  $Q^{-1}$  peaks at about 240 K and with no modulus hysteresis when there is no  $Q^{-1}$  anomaly at 240 K. The absence of these effects in some specimens is probably attributable to particular grain size and internal stress distributions, Figures 4; references 25.

**New Conformal Theories, "Magic" Level  $k = 4$ ,  
and Integrable Models**

917J0016A Moscow PISMA V ZHURNAL  
EKSPERIMENTALNOY I TEORETICHESKOY  
FIZIKI in Russian Vol 52 No 5, 10 Sep 90 pp 888-889

[Article by A. A. Belov and Yu. Ye. Lozovik, Institute of Spectroscopy, USSR Academy of Sciences]

[Abstract] Inasmuch as multiparametric properties of families of conformal theory surfaces, in connection with the theory of strings have not yet been established, a new approach is taken by seeking a relation between these surfaces and exactly solvable Turbiner models in quantum mechanics and by demonstrating the existence of multiparametric solutions to the Virasoro conditions. For the  $SO(d)_k$  algebra with  $k = 4$ , moreover, conformal theories are shown to form a  $D$ -dimensional ( $D = d - 2$ )

surface in the  $R^{2D}$  space of parameters of integrable models. Substitution of the diagonal ansatz for these algebras in the system of Virasoro conditions will yield a homogeneous system of  $[d(d - 1) / 2] - 1$  independent cubic equations for the  $S_{\alpha\beta}$  coefficients. The number of these coefficients is equal to the number of equations in the system, and the latter generally has only a discrete set of solutions, multiparametric families of solutions are possible only when  $k =$  "magic" 4. After the degrees of freedom have been appropriately reparametrized so that only 2D independent parameters remain, dynamic systems on  $SO(d)$  algebras with the Hamiltonian  $H = \sum S_{\alpha\beta} J^{\alpha\beta} J^{\alpha\beta}$  are completely integrable and it thus becomes possible to describe conformal theory surfaces by Morozov's generalized homeomorphic conformal mapping. It is further demonstrated that  $\dim M_{VIR} = D$ , but it still remains to be determined owing to which of their "intensive" property integrable models can be "elevated" to conformal theories. References 4.

UDC 517.94

**Analog of Newton's Diagram for Class of Differential Equations With Singular Perturbation: Part 2**

917J0007A Minsk DIFFERENTIALNYE  
URAVNENIYA in Russian Vol 26 No 9, Sep 90  
pp 1500-1509

[Article by G. S. Zhukova, Moscow Institute of Chemical Engineering imeni D. I. Mendeleev]

[Abstract] The differential vector equation  $\varepsilon^h dx / dt = A(t, \varepsilon)x$  is considered where  $\varepsilon$  is a small real parameter within the range  $(0, \varepsilon_0]$  and  $h$  is a natural number. On the interval  $[0, T]$  of time  $t$  the matrix function  $A(t, \varepsilon)$  has a uniform asymptotic representation  $A(t, \varepsilon) \rightarrow A_0(t) - \sum_{s=1}^{\infty} \varepsilon^s A_s(t)$  over all  $s \leq 1$  as  $\varepsilon \rightarrow +0$  and  $A_0$  has an isolated identically multiple eigenvalue of algebraic multiplicity  $n$  and geometric multiplicity  $m$ , both  $n$  and  $m$  not depending on time  $t$ . While the matrix  $A(t, \varepsilon)$  is an  $n \times n$ -dimensional, one with real coefficients continuous in time throughout the interval  $[0, T]$ , the matrix  $A_s(t)$  ( $s \leq 1$ ) is an  $n \times n$ -dimensional, one with real coefficients infinite times differentiable with respect to time  $t$ . The limiting operator in the expansion does not depend on time  $t$  and is in space  $R^n$  determined by the matrix  $A_0 = \text{diag}(\Lambda_1, \dots, \Lambda_m)$  ( $1 \leq m \leq n - 1$ ), where  $\Lambda_s$  is an  $n_s$ -dimensional Jordan cage and  $n_1 + \dots + n_k = n$ . The solution to this equation is sought in the form of an  $n$ -dimensional vector function  $x(t, \varepsilon)$  with coordinates in the class of formal series in terms of any asymptotic sequence  $[\varepsilon^{r(s)}]$  and coefficients from the set  $C^\infty [0, T]$  which satisfy the equality  $\varepsilon^h dx(t, \varepsilon) / dt = [A_0(t) - \sum_{s=1}^{\infty} \varepsilon^s A_s(t)]x(t, \varepsilon)$  on the interval  $[0, T]$ . Following validation of auxiliary constructions with a theorem aided by a

lemma and subsequent redefinition of the problem, more precisely for the one-dimensional case (one-dimensional Jordan cage), the analog of Newton's diagram is applied for obtaining such formal solutions in accordance with two validating theorems. The procedure is then outlined in four steps. The solution by this procedure is demonstrated on two special cases, with the support of a validating theorem for each. References 15.

UDC 517.977.8

**Class of Linear Differential and Discrete Games Between Groups of Pursuers and Evaders**

917J0007B Minsk DIFFERENTIALNYE  
URAVNENIYA in Russian Vol 26 No 9, Sep 90  
pp 1541-1551

[Article by N. Yu. Satimov and M. Sh. Mamatov, Tashkent State University imeni V. I. Lenin]

[Abstract] A differential game between a group of pursuers and a group of evaders describable by the system of two equations  $dx_i / dt = \alpha_i x_i + \rho_i u_i$  and  $dy_j / dt = \beta_j y_j + \sigma_j v$  is considered where  $x_i, y_j$  are in  $R^n$ -space,  $\alpha_i, \beta_j$  are in  $R^1$ -space and  $\rho_i, \sigma_j \leq 0$  are in  $R^1$ -space,  $|u_i| \leq 1$  (pursuers' control parameter) and  $|v| \leq 1$  (evaders' control parameters). Three theorems are proved for such a game, one theorem stating two conditions under which capture within a given time is possible and two theorems each stating a condition under which escape is possible. The discrete analog of such a game is described by the system of two recurrence equations  $x_i(v+1) = \alpha_i x_i(v) + \rho_i u_i(v)$  ( $i = 1, 2, \dots, m$ ) and  $y_j(vn+1) = \beta_j y_j(v) + \sigma_j v(v)$  ( $j = 1, 2, \dots, k$ ) is then considered where  $v$  is the consecutive number of a step. References 14.

22161

SPRINGFIELD, VA  
5285 PORT ROYAL RD  
ATTN: PROCESS 103  
NTIS

21  
22161

This is a U.S. Government publication containing political, military, economic, environmental, and sociological news, commentary, and other information, as well as scientific and technical data and reports. All information has been obtained from foreign radio and television broadcasts, news agency transmissions, newspapers, books, and periodicals. Items generally are processed from the first or best available sources. It should not be inferred that they have been disseminated only in the medium, in the language, or to the area indicated. Items from foreign language sources are translated; those from English-language sources are transcribed. Except for excluding certain diacritics, FBIS renders personal and place-names in accordance with the romanization systems approved for U.S. Government publications by the U.S. Board of Geographic Names.

Foreign Broadcast Information Service (FBIS) and Joint Publications Research Service (JPRS) publications contain political, military, economic, environmental, and sociological news, commentary, and other information, as well as scientific and technical data and reports. All information has been obtained from foreign radio and television broadcasts, news agency transmissions, newspapers, books, and periodicals. Items generally are processed from the first or best available sources. It should not be inferred that they have been disseminated only in the medium, in the language, or to the area indicated. Items from foreign language sources are translated; those from English-language sources are transcribed. Except for excluding certain diacritics, FBIS renders personal and place-names in accordance with the romanization systems approved for U.S. Government publications by the U.S. Board of Geographic Names.

Headlines, editorial reports, and material enclosed in brackets [ ] are supplied by FBIS/JPRS. Processing indicators such as [Text] or [Excerpts] in the first line of each item indicate how the information was processed from the original. Unfamiliar names rendered phonetically are enclosed in parentheses. Words or names preceded by a question mark and enclosed in parentheses were not clear from the original source but have been supplied as appropriate to the context. Other unattributed parenthetical notes within the body of an item originate with the source. Times within items are as given by the source. Passages in boldface or italics are as published.

#### SUBSCRIPTION/PROCUREMENT INFORMATION

The FBIS DAILY REPORT contains current news and information and is published Monday through Friday in eight volumes: China, East Europe, Soviet Union, East Asia, Near East & South Asia, Sub-Saharan Africa, Latin America, and West Europe. Supplements to the DAILY REPORTs may also be available periodically and will be distributed to regular DAILY REPORT subscribers. JPRS publications, which include approximately 50 regional, worldwide, and topical reports, generally contain less time-sensitive information and are published periodically.

Current DAILY REPORTs and JPRS publications are listed in *Government Reports Announcements* issued semimonthly by the National Technical Information Service (NTIS), 5285 Port Royal Road, Springfield, Virginia 22161 and the *Monthly Catalog of U.S. Government Publications* issued by the Superintendent of Documents, U.S. Government Printing Office, Washington, D.C. 20402.

The public may subscribe to either hardcover or microfiche versions of the DAILY REPORTs and JPRS publications through NTIS at the above address or by calling (703) 487-4630. Subscription rates will be

provided by NTIS upon request. Subscriptions are available outside the United States from NTIS or appointed foreign dealers. New subscribers should expect a 30-day delay in receipt of the first issue.

U.S. Government offices may obtain subscriptions to the DAILY REPORTs or JPRS publications (hardcover or microfiche) at no charge through their sponsoring organizations. For additional information or assistance, call FBIS, (202) 338-6735, or write to P.O. Box 2604, Washington, D.C. 20013. Department of Defense consumers are required to submit requests through appropriate command validation channels to DIA, RTS-2C, Washington, D.C. 20301. (Telephone: (202) 373-3771, Autovon: 243-3771.)

Back issues or single copies of the DAILY REPORTs and JPRS publications are not available. Both the DAILY REPORTs and the JPRS publications are on file for public reference at the Library of Congress and at many Federal Depository Libraries. Reference copies may also be seen at many public and university libraries throughout the United States.